

© This manuscript version is made available under the CC-BY-NC-ND 4.0 license
<https://creativecommons.org/licenses/by-nc-nd/4.0/>

The definitive publisher version is available online at [10.1016/j.desal.2022.115951](https://doi.org/10.1016/j.desal.2022.115951)

Metal-based adsorbents for lithium recovery from aqueous resources

Hanwei Yu¹, Gayathri Naidu¹, Chunyao Zhang², Chen Wang¹, Amir Razmjou^{3,1}, Dong Suk Han⁴,
Tao He², Hokyong Shon^{1,*}

¹School of Civil and Environmental Engineering, University of Technology Sydney (UTS), City
Campus, Broadway, NSW 2007, Australia

²Laboratory for Membrane Materials and Separation Technologies, Shanghai Advanced Research
Institute, Chinese Academy of Sciences, Shanghai 201210, China

³School of Engineering, Edith Cowan University, Joondalup, Perth, WA 6027, Australia

⁴Center for Advanced Materials & Department of Chemical Engineering, Qatar University, P.O.
Box 2713, Doha, Qatar

*Corresponding author email: Hokyong.Shon-1@uts.edu.au

Abstract

The continuous increase of demand for lithium (Li) chemicals in industrial applications calls for exploring affordable Li production and sustainable options beyond land mining. Thus, aqueous resources, such as geothermal brine, salt lake brine, and seawater, play an essential role in continuous Li supply due to abundant storage and low cost. Adsorption technology is promising in Li recovery with the advantages of attaining high selectivity for Li over other major ions present in aqueous resources at low cost and low energy demand with facile synthesis processes that enable practical large-scale production. Metal-based adsorbents are conspicuous among various adsorbents for presenting the visible prospect closest to industrial applications. This review presents a comprehensive summary and critical analysis of the synthesis methods for metal-based adsorbents, the mechanisms for Li selective recovery, and the performance of Li adsorption. The

25 advantages and challenges are discussed for different adsorbents and preparation methods. A
 26 specific focused case study on an industrial application of Al-based adsorbent production and Li
 27 recovery processes and operations on an engineering and economic scale is discussed in detail to
 28 provide a comprehensive overview of the practical industrial application of metal-based adsorbent.

29

30 **Keywords**

31 Lithium recovery; Metal-based adsorbents; Adsorption performances; Synthesis methods;
 32 Industrial case study

33

34 **Table of Content**

35 Highlights..... **Error! Bookmark not defined.**
 36 Abstract 1
 37 Graphical Abstract..... **Error! Bookmark not defined.**
 38 Keywords 2
 39 Table of Content 2
 40 1. Introduction 4
 41 2. Metal-based Li adsorbents 9
 42 2.1 Al-based adsorbents 9
 43 2.1.1 Structure and adsorption mechanism 9
 44 2.1.2 Synthesis methods and Li recovery performances 11
 45 2.2 Mn-based adsorbents 13
 46 2.2.1 Type, structure, and adsorption mechanism 13
 47 2.2.2 Synthesis methods and Li recovery performance 15
 48 2.3 Ti-based adsorbents 19
 49 2.3.1 Type, structure, and adsorption mechanism 19
 50 2.3.2 Synthesis methods and Li recovery performance 21
 51 2.4 Comparison of three types of metal-based Li adsorbents 26
 52 3. Case study - Application of metal-based adsorbent for Li recovery in an actual industrial site 28
 53 3.1 Adsorbent production and regeneration technologies 28
 54 3.2 Li recovery process and operation 29

55	3.3 <i>Cost, benefit, and economic evaluation</i>	31
56	4. Outlook and Conclusions	32
57	Declaration of competing interest	33
58	Acknowledgment.....	34
59	References	34
60		
61		

62 **1. Introduction**

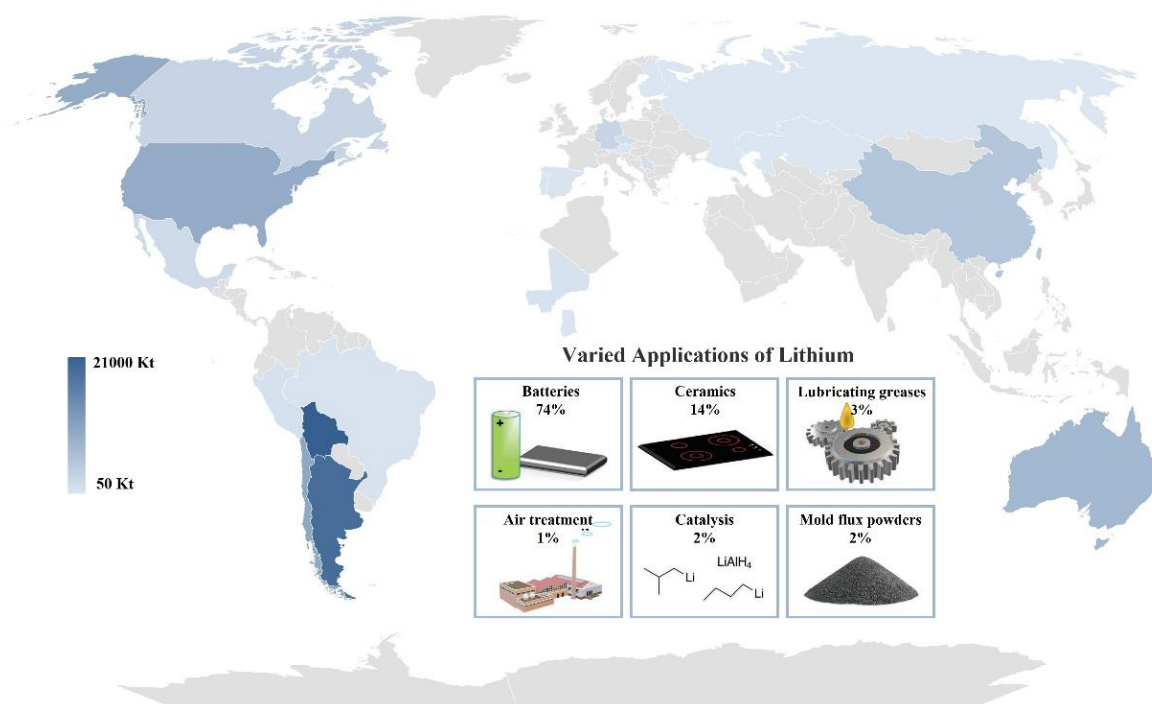
63 Lithium (Li) has become one of the most crucial elements in this century in various industries
64 because of its electrochemically active property and high specific heat capacity [1, 2]. **Fig. 1** shows
65 diverse applications and distribution of identified Li resources on land. **Fig. 2** presents annual Li
66 consumption from 2010 to 2020 and the distribution of extractable Li reserves with existing
67 technologies [3-9]. The applications cover batteries, ceramics, lubricating greases, air treatment,
68 catalysis, etc. Notably, in recent five years, the expansion of batteries for electric vehicles and other
69 electric devices has been accelerated rapidly by the concept and policies of replacing traditional
70 fuel energy to clean renewable energy in many countries [9-11]. The boom of global Li
71 consumption, from 24.5 kt in 2010 to 93.0 kt in 2021 [4], challenges the supply of Li from
72 conventional ore resources. On that note, recovering Li from aqueous sources exhibits significant
73 advantages as an alternative Li resources, as about 75% of Li on land is stored in geothermal brines,
74 oilfield brines, and the salt lakes in South America, China, and Australia [12], and the reserve in
75 the ocean is even over 16 thousand times than that on land [9].

76 The main approaches to extracting Li from brines include conventional evaporation
77 precipitation [13], solvent extraction [14-16], and adsorption [17], and emerging technologies such
78 as electrochemical methods [18-22], membrane-based technologies [14, 23-27], and reaction-
79 coupled separation [28]. The predominant factors that influence selecting a method for Li
80 extraction are the practical applicability of the method, the co-existing contaminant multivalent
81 cations (namely the Mg/Li mass ratio), and the effects of other competing co-existing ions, such as
82 Na^+ , K^+ [29-32]. The widely used evaporation precipitation method is limited to applying in the
83 high Mg/Li ratio brines due to the complex and time-consuming pre-processes of removing co-
84 existing ions [12, 33, 34]. The solvent extraction method for extracting Li from multi-ion-existing

85 brines shows undesirable sustainability since the organic solvents can corrode the process
86 equipment and the solvent leakage pollutes the environment [35, 36]. Electrochemical Li capture
87 systems [37], including capacitive deionization (CDI) [38-40] and electrodialysis (ED) [41-44]
88 based on electrochemically switchable ion exchange (ESIX) rely on the external electric field, thus
89 being limited by problems of high cost and energy consumption. Membrane-based technologies
90 for Li recovery contain capacitive deionization (MCDI) [45-47], selective electrodialysis (SED)
91 [21, 26, 32, 44], nanofiltration (NF) [24, 48], ion-imprinted membrane (IIM) [49, 50], and
92 membrane distillation crystallization (MDC) [51, 52], driven by external stimuli such as thermal
93 gradient, pressure, and electric field [53-57]. These technologies have vast potential to develop in
94 the next generation roadmap, yet the difficulties of energy consumption, separation efficiency, and
95 membrane durability limit their industrialization. Reaction-coupled separation technology for the
96 separation of Mg/Li by co-precipitating Mg-ions and foreign Al-ions with an alkali solution is still
97 at the start-up stage [28, 29].

98 Compared to the above technologies, the adsorption method shows an excellent balance of
99 high Li selectivity, simple and efficient operation process, good applicability to most brine
100 resources, high economical advantage, and less environmental impact [58, 59]. It utilizes Li-
101 selective adsorbents to uptake Li from a multi-ion aqueous environment and then desorbs them
102 with some solvents, thus extracting Li. The principle requirements for proper adsorption materials
103 cover high Li selectivity, adequate adsorption capacity, and suitable operation stability [60]. As
104 shown in **Fig. 3**, the mainly studied Li adsorbents involve inorganic, organic, and composite
105 adsorbents. Organic adsorbents, such as crown ether and polymer ion-exchange resin, are limited
106 for applications due to the hazardous organic raw materials and the complex synthesis processes.
107 Inorganic adsorbents include metal-based adsorbents and natural mineral-based adsorbents. The

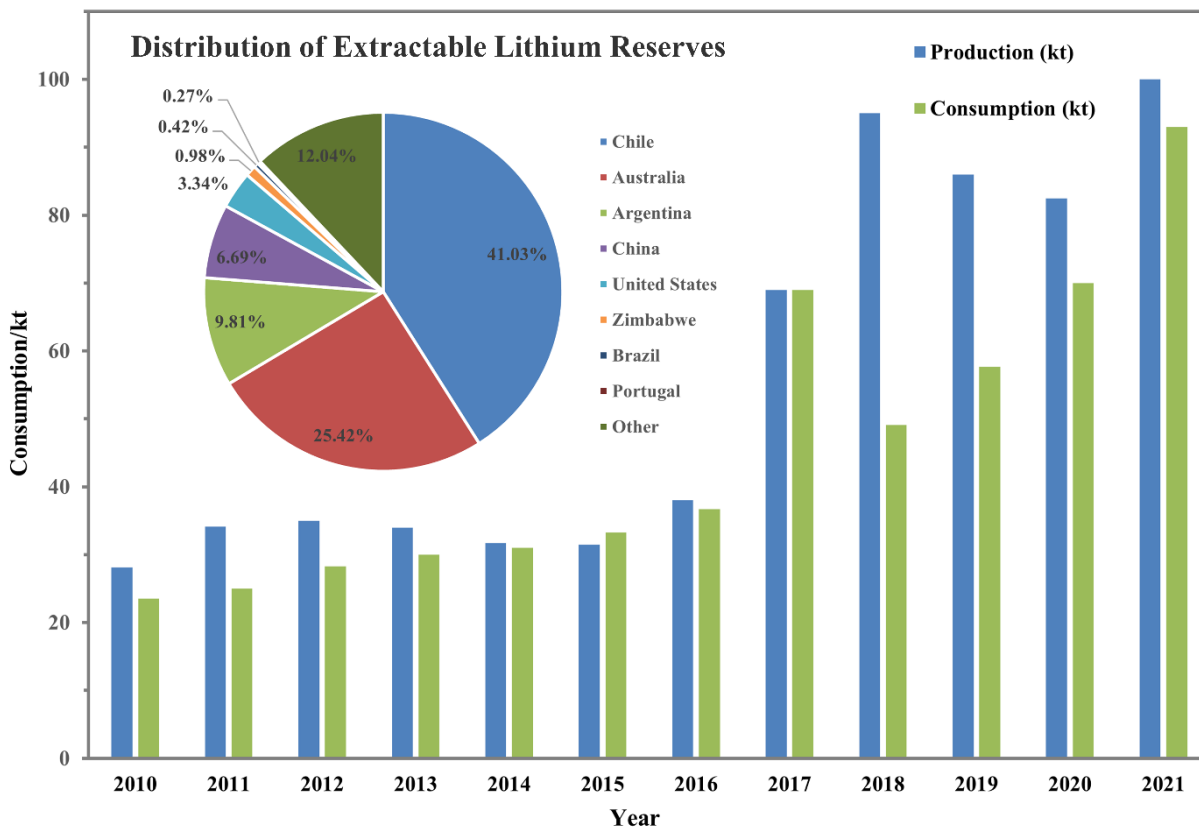
108 selection of the latter ones strongly depends on cost and resource quantity, impeding promoted
109 applications in different brine source areas. Nowadays, metal-based adsorbents have
110 become the hotspot and keystone of the research on Li adsorbents. The merits of metal-based Li
111 adsorbents, including high Li capture capacity, low regeneration loss of raw materials, excellent
112 Li selectivity, robust cycle performance, and relatively less energy consumption, qualify them as
113 promising environmentally-friendly candidates for Li extraction from aqueous solutions
114 containing different ions [61]. The pilot- and commercial-scale applications have been developed
115 in Li recovery cases from the Qarhan Salt Lake by Qinghai Lakelithium Co., LTD. The related
116 case study is developed in Section 3.



117
118 **Figure 1.** Diverse applications of Li and distribution of identified Li resources on land, including
119 exploitable and unexploitable with existing technologies. Figure partly modified from [8] with
120 copyright permission from John Wiley and Sons.

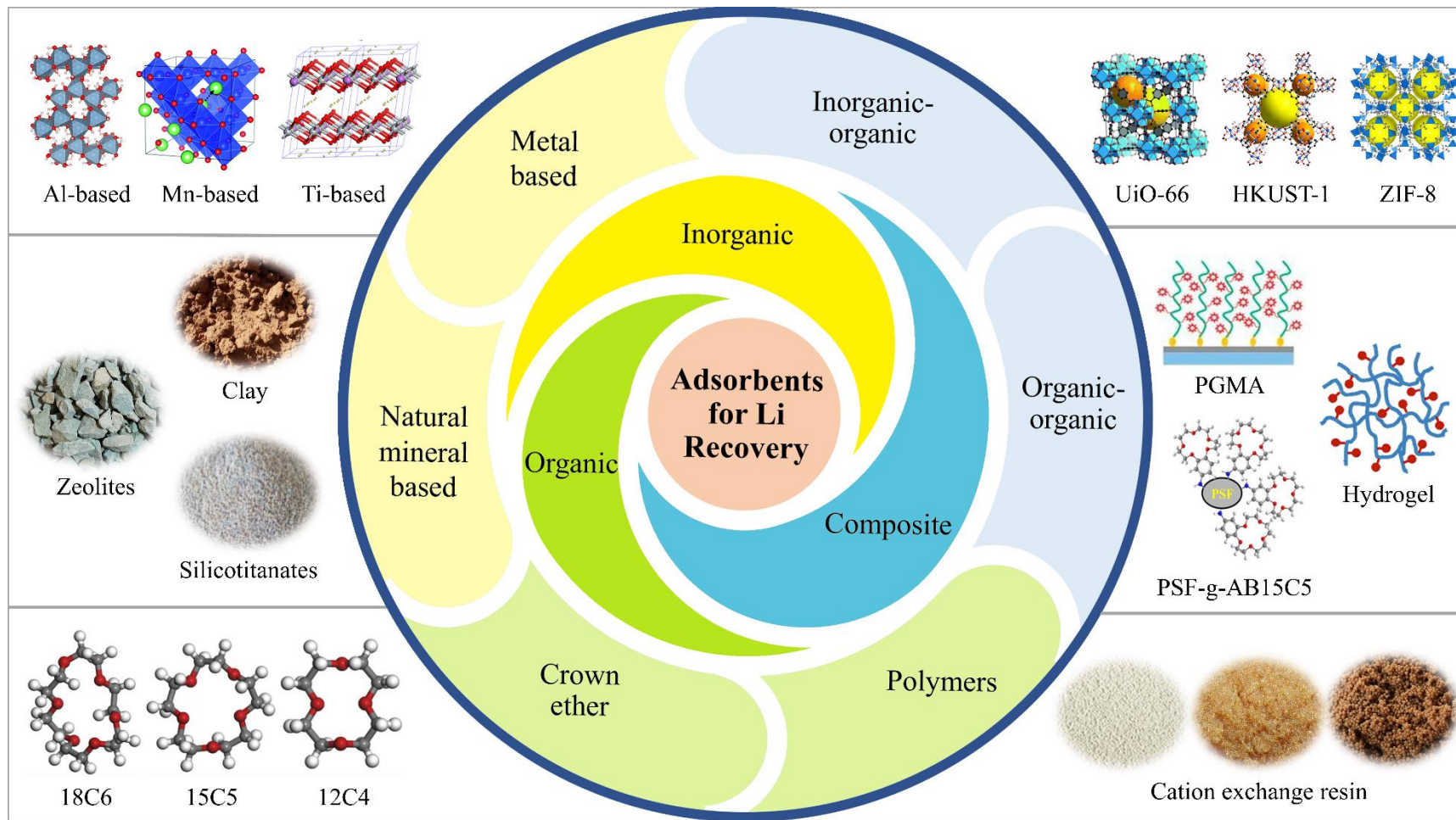
121 Previous review papers on Li recovery focused on 1) membrane-based [14], manganese-
122 based [62], and MOF-based [8] Li extraction materials, 2) electrochemical methods [18, 41, 63],

123 and other industry production methods [64, 65] from one specific brine source [13, 66] or region
 124 [67], 3) brine and mineral management perspectives [68, 69]; however, thus far, almost no
 125 comprehensive reviews concerning the developments of all metal-based adsorbents for Li recovery
 126 from sorts of brines. This review emphasizes the synthesis methods and Li adsorption
 127 performances of the current and the emerging metal-based Li adsorbents. Simultaneously, the
 128 techno-economic analysis is studied based on the application case of Al-based adsorbent in Li
 129 recovery from the Qarhan Salt Lake. The challenges and potential opportunities to implement on
 130 the future engineering scale are also discussed.



131
 132 **Figure 2.** Global consumption of Li content from 2010 to 2020 and distribution of extractable Li
 133 reserves with existing technologies.

134
135
136



137

138 **Figure 3.** Classification of adsorbents for Li recovery.

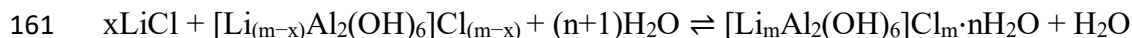
139 2. Metal-based Li adsorbents

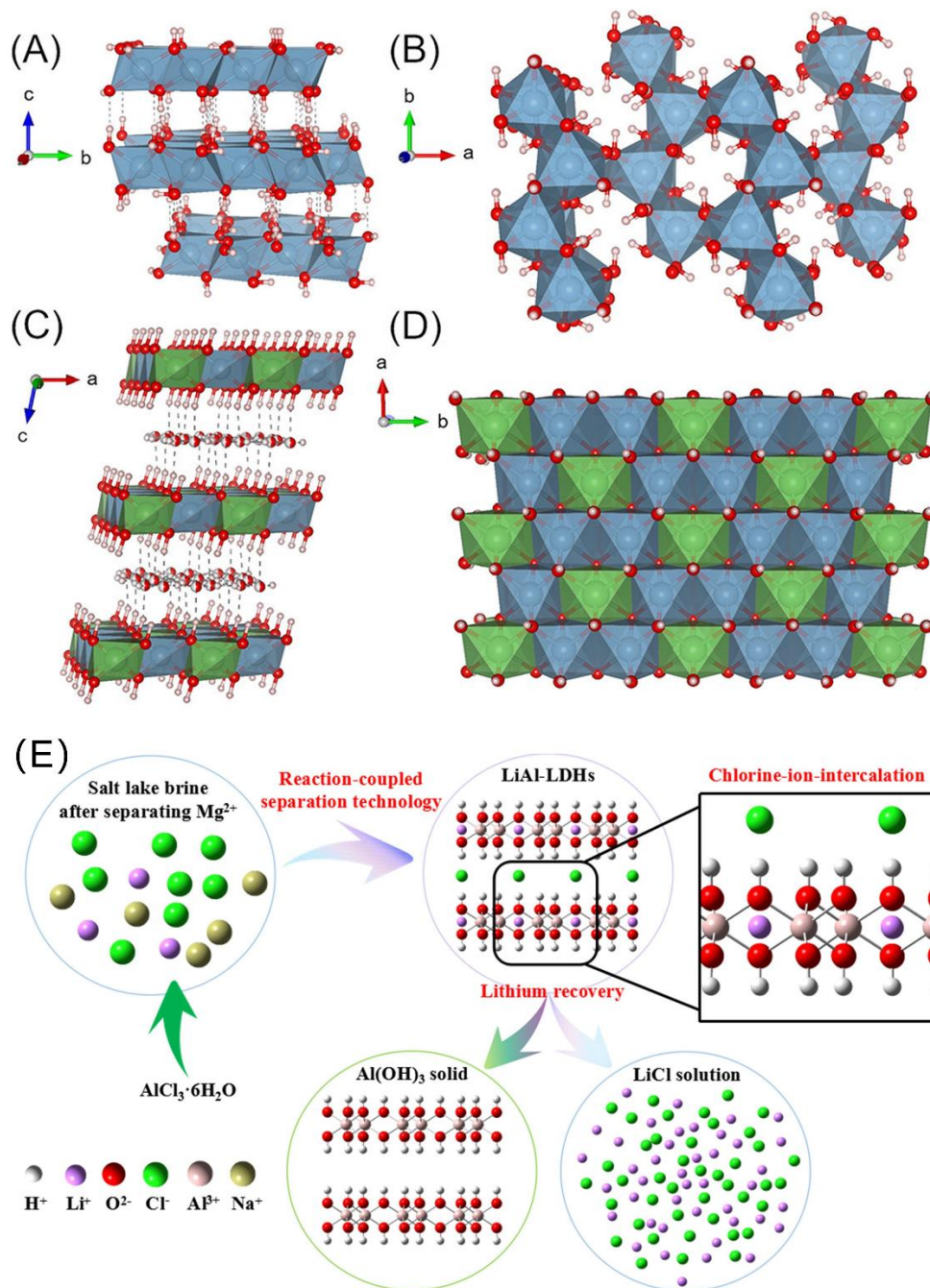
140 Metal-based Li adsorbents for Li recovery are basically comprised of aluminum (Al)-based,
141 manganese (Mn)-based, and titanium (Ti)-based adsorbents. The overarching principle governing
142 Li sorption by metal adsorbents is based on the structural memory effect of Li-ion sieves (LIS): Li
143 tends to occupy the vacancies generated in the adsorbent preparation process by removing the
144 original Li from the pristine structure [70-72]. For now, Al-based adsorbents exhibit the most
145 potential in industrial application owing to the high technology maturity, yet the Li selective uptake
146 performance is not ideal; Mn-based ones present excellent Li adsorption performances, but the Mn
147 dissolution impairs its long-term stable application; Ti-based ones is a more recent entry but have
148 shown promising prospects as it does not exhibit the similar disadvantages of the Al-based and
149 Mn-based adsorbents.

150 2.1 Al-based adsorbents

151 2.1.1 Structure and adsorption mechanism

152 Al-based adsorbents, especially Li-Al layered double hydroxides (LiAl-LDHs), are widely
153 studied inorganic adsorbents and the most applicable ones for industrial Li recovery from brines
154 owing to the advantages of negligible elution damage, stable adsorption performance, and ease of
155 production [71, 73]. LiAl-LDHs show a structure of a two-dimensional aluminum hydroxide
156 layered plate linked by hydrogen bonds, electrostatic interaction, and van der Waals with Li filled
157 in octahedral voids of the packing hydroxide ions (**Fig. 4**), and the chemical formula could be
158 expressed as $[\text{Li}_m\text{Al}_2(\text{OH})_6]\text{Cl}_m \cdot n\text{H}_2\text{O}$ ($m=0-1$) [70, 74-76]. Based on the mechanism of the
159 structural memory effect, the process of Li adsorption-desorption can be described as the following
160 formula [73]:





162

163 **Figure 4.** Crystal structures of gibbsite (A, B) and LiAl-LDH (C, D); the blue, red, green, and

164 white dots represent Al, O, Li, and H atoms, respectively. (E) Flowchart for Li recovery from LiAl-

165 LDHs via a mild solution chemistry process. Figure (A-D) obtained from [77] with copyright

166 permission from ACS Publications. Figure (E) obtained from [78] (copyright 2019 MDPI).

167 2.1.2 Synthesis methods and Li recovery performances

168 The synthesis of LiAl-LDHs has a more extended history than the application studies in Li
169 recovery. The Li intercalation method was reported to modify aluminum hydroxide by Frenkel et
170 al. in 1980 [79]. The preparation method of lithium dialuminate using solid lithium hydroxide,
171 polycrystalline aluminum trihydroxide (bayerite), and water vapor at room temperature was
172 described by Poeppelmeier and Hwu in 1987 [80]. The mechanochemical process of LiAl-LDHs
173 production was developed by combining grinding followed by hydrothermal crystallization [81-
174 83]. Isupov et al. proposed using LiAl-LDH as a selective sorbent of Li salts from brines in 1998
175 [84], yet few studies emphasized the application of Li recovery until recent years. Liu et al.
176 produced $\text{LiCl} \cdot 2\text{Al}(\text{OH})_3 \cdot x\text{H}_2\text{O}$ and investigated the Li/Mg separation performance of LiAl-LDH
177 in brine, revealing the ability of LiAl-LDHs to extract Li from the salt lake brine [85]. Zhong et al.
178 prepared two-dimensional hexagonal flat Li/Al-LDHs with high Li selectivity via the
179 coprecipitation method and developed a granulation method to adsorb Li from the Qarhan Salt
180 Lake old brine at room temperature [73, 86]. Lee et al. synthesized silicon oxide-coated LiAl-LDH
181 nanocrystals with stable regeneration cycles and high Li selectivity by oxidation of aluminum foil
182 substrate under a urea and Li solution to extract Li from simulated solution resources [87]. Sun et
183 al. exploited the hybrid technology of reaction-coupled separation and LiAl-LDHs to extract Li
184 from the salt lake brine in the Chinese Qaidam Basin, achieving as low as 3.93% Li loss [88]. Lee
185 et al. proposed a project to separate Li from urea solution using LiAl-LDH coated aluminum metal
186 foils [89] and fabricated polyacrylonitrile hybrid membranes coated with aluminum hydroxide for
187 separating Li [90].

188 For optimal application condition study and large-scale process design, Jiang et al. tested Li
189 adsorption performances of LiAl-LDHs from simulated brine with various initial Li concentrations
190 in different feed flow rates at 303 K in fixed-bed columns with varying heights of bed. Their results

191 indicate that the breakthrough time (the life span of adsorbents in a single adsorption operation)
192 and capacity positively correlate with bed height but negatively with the initial Li concentration
193 and feed flow rate [91], and the optimal pH condition is ascertained to 7 [92, 93]. Paranthaman et
194 al. designed an economic three-stage bench-scale column extraction process, presenting the merits
195 of low cost, easy preparation, and environmentally friendly nature for Li recovery from geothermal
196 brine using LDHs [94]. The competitive and synergic effects of co-existing ions on Li adsorption
197 are concerned in multi-salt feed solutions. Jiang et al. verified the promotion effect of anions and
198 the competition effect of other cations on the Li adsorption through adsorption tests in the Li-
199 MgCl₂, Li-NaCl, and Li-Na-MgCl₂ multicomponent system [17]. Similar investigations were also
200 studied by Chen et al. [71], and Hu et al. [95]. The selectivity factor can be used to compare the Li
201 adsorption ability in the multi-cation environment.

202 Despite the significant advantages in Li extraction from low-grade brines, the drawback of
203 using LiAl-LDHs is that its sensitivity towards transforming to gibbsite in the desorption process
204 reduces its adsorption capacity, which is a major challenge for application scale expansion [93,
205 95]. Prolonging the application life of LiAl-LDHs is also vital to reducing environmental impact
206 [96]. Introducing magnetic materials is a strategy to reduce the sharp loss in the industrial
207 application of adsorption capacity due to granulation as an external magnetic field can be employed
208 after adsorption to recycle adsorbents [97, 98]. Fe₃O₄-doped magnetic LiAl-LDHs are proved not
209 harmful to the physicochemical properties of the effective adsorption component and can achieve
210 rapid recovery and long-term recycling potential [71, 99]. Additionally, except for solid-state
211 intercalation, the dissolution-reprecipitation pathway was also discovered in the transformation
212 from gibbsite to LiAl-LDHs, hinting at another potential study direction on the structural
213 adjustment for reducing effective content loss [77].

214 Except for LiAl-LDHs, other Al-based adsorbents are also reported. Pauwels et al.
 215 investigated Li adsorption of polymeric aluminum hydroxide for geothermal water treatment in
 216 1995 [100]. Wang et al. synthesized magnesium-aluminum-carbonate-layered double hydroxide
 217 adsorbent (MgAlCO₃-LDHs) and developed an integrated process to separate and recover both
 218 Mg and Li from brines [101]. Heidari and Momeni utilized AlCl₃·6H₂O as an adsorbent to recover
 219 Li from Urmia Lake and identified the optimal pH and temperature conditions [102]. In summary,
 220 the synthesis methods and performances of Al-based adsorbents are presented in **Table 1**.

221 **Table 1.** Synthesis methods and performances of Al-based adsorbents

Adsorbents	Sources	Preparation	Li adsorption performance	Ref.
Al(OH) ₃	AlCl ₃ ·6H ₂ O, NaOH, brine	Coprecipitation	Li recovery rate of 76.4% when T=30°C, pH= 7.5	[102]
Al(OH) ₃	AlCl ₃ ·6H ₂ O, KOH, LiCl	Coprecipitation	Li recovery rate of 95% when T=80°C and Al/Li molar ratio ~2.5	[100]
Li/Al-LDHs	LiCl, AlCl ₃ , NaOH	Coprecipitation	Li capacity of 7.27 mg/g in Qarhan old brine	[73]
Li/Al-LDHs	AlCl ₃ ·6H ₂ O, NaOH, brine	Coprecipitation	Li recovery rate of 89.7% when T=30°C and Al/Li =5	[103]
Li/Al-LDHs	LiCl, NaOH, AlCl ₃ ·6H ₂ O	Coprecipitation	Li capacity of 6 mg/g	[71]
Li/Al-LDHs	Al(OH) ₃ , LiOH·H ₂ O, HCl	Hydrothermal method	Li recovery rate of 91%	[94]
Li/Al-LDHs	LiCl, AlCl ₃ , NaOH		Li capacity is about 3 mg/g	[104]
Li/Al-LDHs	AlCl ₃ ·6H ₂ O, NaOH, Na ₂ CO ₃		3.93% Li loss under optimal separation conditions	[88]
Li/Al-LDHs	AlCl ₃ ·6H ₂ O, LiOH·H ₂ O, NaOH	Coprecipitation	Li capacity of 9.33 mg/g	[93]
Commercial adsorbent	/	/	Li capacity range of 5.02 to 5.69 mg/g from 200 to 350 mg/L initial LiCl solution	[17]

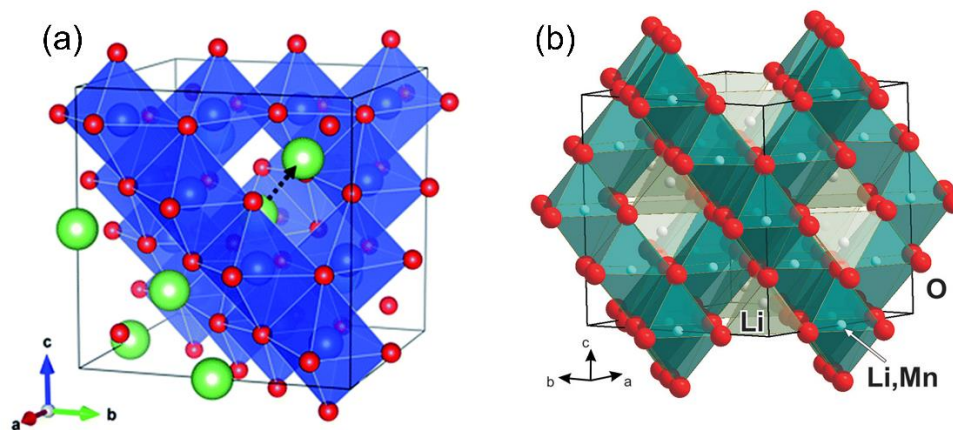
222

223 2.2 Mn-based adsorbents

224 2.2.1 Type, structure, and adsorption mechanism

225 Mn-based adsorbents (LMO) are broadly emphasized in research due to their unique chemical
 226 structure, sufficient adsorption capacity, excellent Li selectivity, and outstanding regeneration
 227 performance [61]. For now, the precursors of LMOs can be divided into three types according to
 228 the different ratios of Li/Mn and crystal structures: LiMn₂O₄, Li_{1.33}Mn_{1.67}O₄ (Li₄Mn₅O₁₂), and

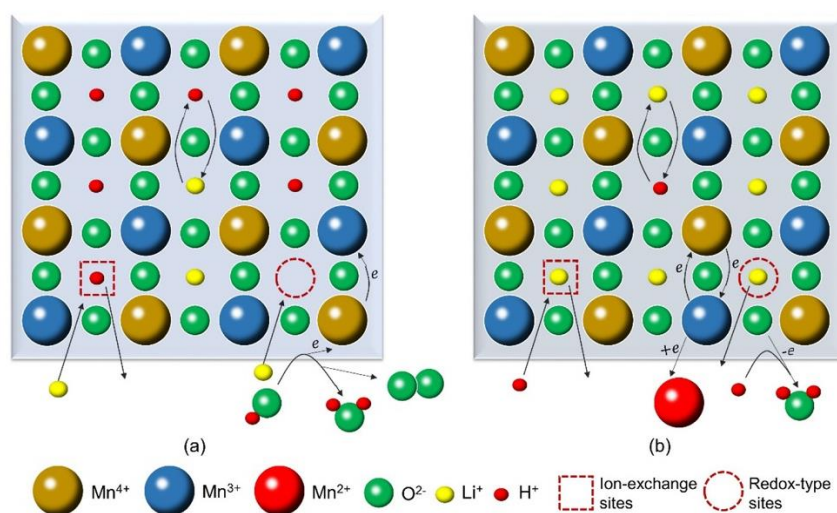
229 $\text{Li}_{1.6}\text{Mn}_{1.6}\text{O}_4(\text{Li}_2\text{Mn}_2\text{O}_5)$, with theoretical maximum adsorption capacities of 39.9 mg/g, 59.5 mg/g
230 and 72.8 mg/g, respectively [105-108]. The crystal structures of $\text{Li}_x\text{Mn}_{3-x}\text{O}_4$ spinels are determined
231 by stoichiometry, applied pressure, and temperature in the solid-phase reaction by heating a
232 mixture of Mn and Li compounds [109]. As **Fig. 5** shows, spinel-based LiMn_2O_4 and $\text{Li}_4\text{Mn}_5\text{O}_{12}$
233 exhibit cubic crystal structures. Li and Mn occupy tetrahedral and octahedral sites of LiMn_2O_4
234 crystal, respectively [110]. On the basis of LiMn_2O_4 , the excessive amount of Li at octahedral sites
235 compensate for the increase of Mn(IV) in $\text{Li}_4\text{Mn}_5\text{O}_{12}$ [111]. The structural model of $\text{Li}_2\text{Mn}_2\text{O}_5$ has
236 not been explicitly reported, but the advantage of its superior theoretical exchange capacity appeals
237 to researchers as a candidate precursor for an ideal Li-selective adsorbent.



238
239 **Figure 5.** Crystal structure of spinel (a) LiMn_2O_4 and (b) $\text{Li}_4\text{Mn}_5\text{O}_{12}$, Mn ions reside in
240 octahedrons formed by O ions. Figure (a) obtained from [112] with copyright permission from
241 Royal Society of Chemistry and figure (b) obtained from [110] with copyright permission from
242 ACS Publications.

243 A number of different mechanism theories of Li intercalation-deintercalation have been
244 reported. In 1981, Hunter et al. proposed that Mn(III) in LiMn_2O_4 converted to Mn(II) and Mn(IV)
245 through redox reaction under acidic conditions, only leaving Mn(IV) in $\lambda\text{-MnO}_2$ and providing

246 vacancies for Li intercalation [113]. The dissolution of Mn(II) can reduce the stability of the spinel,
 247 so adsorption capacity decreases with regeneration. But this theory was unable to explain the
 248 phenomenon of the positive influence of the adsorption capacity with pH. A follow-up study by
 249 Shen and Clearfield in 1986 stated that ion exchange between H and Li provided Li vacancies
 250 rather than the disproportionation reaction of Mn ions [114, 115]. Ooi et al. and Feng et al.
 251 concluded the two theories and investigated the Li intercalation process in different types of Mn-
 252 based ion-sieves, discovering that Mn(III) in the precursors deliver redox sites and Mn(IV) grant
 253 ion-exchange sites (shown in **Fig. 6**) [116, 117].



254
 255 **Figure 6.** Schematic representation of the Li intercalation (a) and deintercalation (b) mechanisms
 256 in spinel LMO adsorbents. Figure obtained from [66] with copyright permission from Elsevier.

257 2.2.2 Synthesis methods and Li recovery performance

258 Traditional methods for synthesizing LMO precursors focus on redox precipitation and solid-
 259 phase calcination that Li and Mn compounds are mixed according to a certain stoichiometric ratio
 260 and calcined at more than 400°C [118]. Sun et al. prepared a spinel $\text{Li}_{1.6}\text{Mn}_{1.6}\text{O}_4$ by a combination
 261 of controlled redox precipitation and solid-phase reaction, and the Li adsorption capacity from
 262 Qarhan Salt Lake brine was 3.88 mmol/g [119]. However, since this strategy exhibits the

263 disadvantages of coarse and uneven sizes and distributions of the product powders, prolonged
264 reaction time, and high reaction temperature, the mechanochemical method [120] and rheological-
265 phase-assisted microwave method [121] were proposed to improve the synthesis processes and
266 products. The mechanochemical method is a mechanical activation method for preparing highly
267 dispersed compounds at room temperature or relatively low temperatures. The rheological-phase-
268 assisted microwave method is a combination of microwave treatment and rheological phase
269 method, an approach to facilitate the uniformity of reactants from a solid-liquid rheological
270 mixture. Then the sol-gel method was introduced to optimize the crystallization process [122]. Sun
271 et al. synthesized spinel LiMn_2O_4 powders using metal acetates containing poly(acrylic acid) (PAA)
272 as a chelating agent [123]. To further simplify the synthesis operation and decrease the cost, the
273 hydrothermal and microwave hydrothermal methods were utilized in LMO precursor production.
274 Different morphologies, including nanorods, nanowire, nanocubes, and nanospheres, can be
275 achieved by controlling hydrothermal conditions [107, 108, 124, 125]. Chitrakar et al. employed
276 monoclinic type $\gamma\text{-MnOOH}$ reacting with LiOH solution at 120°C for 24 hours, giving
277 orthorhombic LiMnO_2 , and then heated to higher than 400°C to form cubic $\text{Li}_{1.6}\text{Mn}_{1.6}\text{O}_4$ [126].
278 Then they exploited microwave irradiation on the materials above, realizing a rapid formation of
279 semicrystalline orthorhombic LiMnO_2 (*o*- LiMnO_2) within 30 minutes [127]. The maximum Li
280 uptake of their adsorbent from seawater was 40 mg/g [128]. Shi et al. examined Li adsorption
281 capacity and stability of $\text{Li}_{1.6}\text{Mn}_{1.6}\text{O}_4$ prepared by a hydrothermal reaction, showing a maximum
282 Li uptake of 27.15 mg/g from brine at 50°C and 20 mg/g after 10 cycles [129]. The cross-linking
283 strategy was employed by Wang et al., who produced ethylene glycol diglycidyl ether
284 (EGDE) cross-linked spherical chitosan- $\text{Li}_4\text{Mn}_5\text{O}_{12}$ with 8.98 mg/g of Li adsorption capacity in
285 geothermal brine [130]. In summary, the synthesis methods and performances of LMO are

286 concluded in **Table 2**.

287 **Table 2.** Synthesis methods and performances of Mn-based adsorbents

Adsorbents	Sources	Preparation	Li adsorption performance	Ref.
$\text{Li}_{1+x}\text{Mn}_{2-x}\text{O}_4$	LiOH, Li_2CO_3 , MnCO_3	Solid-phase method	23.5 mg/g in mixed solution within 24 h	[131]
$\text{Li}_{1.6}\text{Mn}_{1.6}\text{O}_4$	$\gamma\text{-MnOOH}$, LiOH	Hydrothermal method	40 mg/g in seawater	[128]
$\text{Li}_{1.6}\text{Mn}_{1.6}\text{O}_4$	KMnO_4 , LiOH, MnCl_2	Hydrothermal method and solid-phase method	28.32 mg/g in Qarhan Salt Lake Li adsorption 3.62 mmol/g after reusing for six cycles.	[108]
$\text{Li}_{1.6}\text{Mn}_{1.6}\text{O}_4$	LiOH, $\text{Mn}(\text{NO}_3)_2$	Hydrothermal method	26.93 mg/g in Qarhan Salt Lake brine	[119]
$\text{Li}_{1.6}\text{Mn}_{1.6}\text{O}_4$	LiOH, Mn_2O_3	Hydrothermal method	27.15 mg/g in brine, Mn loss <2.5%, capacity >20 mg/g after 10 cycles	[129]
$\text{Li}_{1.353}\text{Mn}_{1.626}\text{O}_4$	$\text{Mn}(\text{NO}_3)_2 \cdot 4\text{H}_2\text{O}$, $\text{Na}_2\text{S}_2\text{O}_8$, LiNO_3	Hydrothermal method	Li recovery rate reaches 90% in Urmia Lake	[132]
$\text{Li}_4\text{Mn}_5\text{O}_{12}$	LiNO_3 , $\beta\text{-MnO}_2$	Hydrothermal method and solid-phase method	45.95 mg/g in the solution with $c(\text{Li}) = 5.0 \text{ mol/L}$	[107]
$\text{Li}_4\text{Mn}_5\text{O}_{12}$	EDTA, LiNO_3 , $\text{Mn}(\text{NO}_3)_2 \cdot 4\text{H}_2\text{O}$, Li_2CO_3 , MnCO_3	EDTA-citrate complexing method	43.1 mg/g in 0.5g/L LiCl solution	[133]
$\text{HZn}_{0.5}\text{Mn}_{1.5}\text{O}_4$	$\text{Zn}(\text{CH}_3\text{COO})_2 \cdot 4\text{H}_2\text{O}$	Solid-phase method	33.1 mg/g in artificial seawater	[134]
$\text{LiAl}_x\text{Mn}_{2-x}\text{O}_4$	$\text{Mn}(\text{NO}_3)_2$, $\text{AlCl}_3 \cdot 6\text{H}_2\text{O}$, $\text{LiOH} \cdot \text{H}_2\text{O}$, H_2O_2	Hydrothermal method	27.66 mg/g in 50mg/L LiOH solution 19.5 mg/g after repeating 5 cycles	[135]
$\text{Li}_{1.6}\text{Mn}_{1.6-x}\text{Cr}_x\text{O}_4$	$\text{LiOH} \cdot \text{H}_2\text{O}$, $\text{Cr}(\text{NO}_3)_3 \cdot 6\text{H}_2\text{O}$	Hydrothermal method	25.5 mg/g in Lop Nor Salt Lake	[136]

288 For improving the feasibility of the practical application, the strategies of doping and coating
 289 are explored to reduce Mn dissolution in an acidic surrounding and enhance the structural stability
 290 of LMO adsorbents [137, 138]. In Qian et al.'s study, the maximum Li uptake capacity of
 291 $\text{Li}_{1.6}\text{Mn}_{1.6}\text{O}_4$ increased from 32.3 to 35.3, 35.4, and 40.9 mg/g, and Mn dissolution reduced from
 292 5.4% to 3.95%, 4.42%, and 2.1% after tracing surface doping Fe^{3+} , Co^{2+} , and Al^{3+} , respectively
 293 [139, 140]. They also asserted that by doping F^- , S^{2-} , the capacity of $\text{Li}_{1.6}\text{Mn}_{1.6}\text{O}_4$ increased from
 294 26.1 to 33.4 and 27.9 mg/g [141]. Their K-gradient doping experiment results reported that Mn
 295 dissolution reduced from 5.4% to 4% [142]. Xue et al. enhanced the Li adsorption capacity to
 296 29.33 mg/g with 6.22% Mn loss by doping Fe_3O_4 via a hydrothermal process [143]. Cao et al. and
 297 Su et al. revealed the influence of Cr-doping content on Mn dissolution and Li adsorption capacity

298 [144]. By doping 1% Cr, the LMO-Cr shows an initial Li adsorption capacity of 31.67 mg/g and
299 Mn dissolution ratio of 2.1%, yet Li adsorption capacity of 25.5 mg/g and Mn dissolution ratio of
300 0.35% after 20 cycles [136]. Bajestani et al. reported a high adsorption capacity of 53.52 mg/g via
301 doping Co^{2+} in LiMn_2O_4 [145], and Chen et al. stated 27.66 mg/g via doping Al^{3+} [135]. Compared
302 to doping studies, coating strategy currently lacks attention. Luo et al. coated $\text{Al}_2\text{O}_3\text{-ZrO}_2$ on
303 LiMn_2O_4 to enhance chemical stability and utilized it as an electrode to capture Li in an
304 electrochemical way, achieving a Li extraction capacity of 49.92 mg/g and Mn dissolution of 0.1%
305 after 30 cycles [146].

306 Process investigations for practical Li recovery applications, such as granulation methods
307 development and adsorption column design, are also studied by many research groups. Hong et al.
308 immobilized spinel HMO on the alpha-Al bead and induced macropores by adding hydrogel beads
309 before calcination, resulting in similar Li adsorption performance to powdery adsorbents from high
310 Li concentration feed solutions and improving the performance from diluted feed solutions [147-
311 149]. Han et al. prepared millimeter-sized spherical LMO foams with a Li adsorption capacity in
312 natural seawater of 3.4 mg/g via foaming, drop-in-oil, and agar gelatin [150]. Ryu et al. designed
313 a continuous flow adsorption column for efficient Li recovery from seawater with LMO, showing
314 a maximum adsorption capacity of 54.65 mg/g [151]. Multi-ion feed solutions, including simulated
315 and real brines, were also employed to test the selectivity of the adsorptions of Li and other cations.
316 Sun et al. synthesized $\beta\text{-MnO}_2$, spinel-type LiMn_2O_4 , and $\text{Li}_4\text{Mn}_5\text{O}_{12}$ via hydrothermal synthesis
317 and solid-state reaction, then utilized these LMO adsorbents to uptake Li from a solution
318 containing Li, Na, K, Mg, Ca ions, indicating that the MnO_2 nanorod had the best Li selectivity
319 [106]. Similar studies were also researched by Wang et al. [152], Ryu et al. [153], Recepoglu et al.
320 [154], Chaban et al. [155], Roobavannan [52], and Xiao et al. [156].

321 Besides directly adsorbing Li from the Li-rich solution, LMO adsorbents are also combined
322 with electrochemical Li recovery methods [45, 46, 157-159]. Mu et al. coated λ -MnO₂ and
323 LiMn₂O₄ on 3D-graphite felt electrodes to produce a novel flow-type electrochemical Li recovery
324 system that extracts Li 75 mg/h per gram LiMn₂O₄ [160]. Siekierka built a negatively polarized
325 electrode with LMO for the CDI system, realizing 32 mg/g LiCl adsorption [47]. Liu et al.
326 developed a new device using the ESIX technique based on λ -MnO₂/LiMn₂O₄ structures, attaining
327 3.5 mmol/g of Li adsorption capacity and lower than 0.05% Mn loss [105].

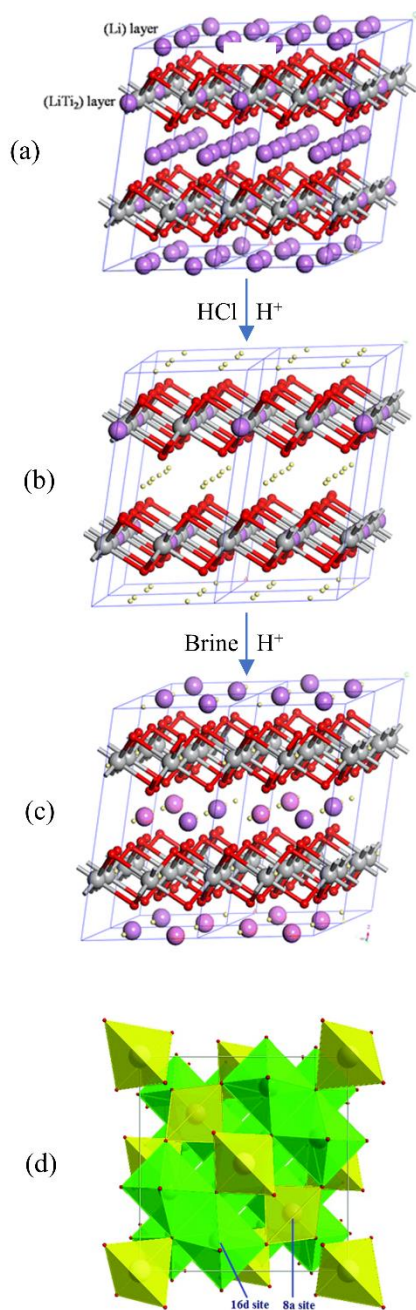
328 *2.3 Ti-based adsorbents*

329 Ti-based adsorbents (LTO) applications for Li recovery have gained momentum in the recent
330 ten years especially due to their stability in acidic solutions. They are considered to be eco-friendly
331 due to their non-reactive leaching propensity to the water environment and easy removal from
332 aqueous solutions [61]. Compared with LMOs, the relatively stable structures of LTOs provide
333 less dissolved loss, high adsorption capacity, excellent selectivity, and recyclability [161, 162].

334 *2.3.1 Type, structure, and adsorption mechanism*

335 The procedure for Li extraction using a Ti-based ion exchanger H₂TiO₃ (HTO) dates from
336 1989, first outlined by Onodera et al., prepared via the acid treatment of HTO [163]. The HTO
337 adsorbent presents a layer crystal structure designated by the Li[Li_{1/3}Ti_{2/3}]O₂. The cell structure,
338 as illustrated in **Fig. 7a**, is a cubic close packing of oxygen atoms accompanied by metal atoms
339 placed in octahedral voids [61, 164, 165]. The exchange of Li and H occurs during the adsorbent
340 preparation, adsorption, and desorption processes. Explicitly speaking, Li is replaced by H in the
341 HTO preparation process by pickling Li₂TiO₃ into hydrochloric acid. Then in the Li extraction
342 process, the memory effect dominates the particular selectivity for accepting Li preferentially
343 because narrow exchange sites left during the preparation reject the occupation of other ions with
344 dissimilar ionic radius or dehydration energy due to steric effects [166]. In a recent study, Marthi

345 et al. proposed a new perspective to the generally accepted ion-exchange mechanism without
346 chemical bond breakage theory. They proposed a new explanation that O–H bonds break and the
347 O–Li bonds form after thermogravimetric analysis, Raman spectroscopy and Fourier transform
348 infrared spectroscopy studies [167]. Except for layer crystal Li_2TiO_3 , spinel $\text{Li}_4\text{Ti}_5\text{O}_{12}$ (**Fig. 7d**), a
349 star candidate of large-scale Li-ion batteries [168], is considered another LTO adsorbent. The
350 mechanisms of Li intercalation and deintercalation are similar to LMO adsorbents, i.e., the redox,
351 ion exchange, and composite mechanisms [61].



352
 353 **Figure 7.** Crystal structure of (a) layered Li_2TiO_3 , (b) H_2TiO_3 , (c) H_2TiO_3 upon Li exchange, and
 354 (d) spinel $\text{Li}_4\text{Ti}_5\text{O}_{12}$. (a), (b), and (c) obtained from [166] with copyright permission from Springer
 355 Nature. (d) from [169] with copyright permission from Royal Society of Chemistry.

356 2.3.2 Synthesis methods and Li recovery performance

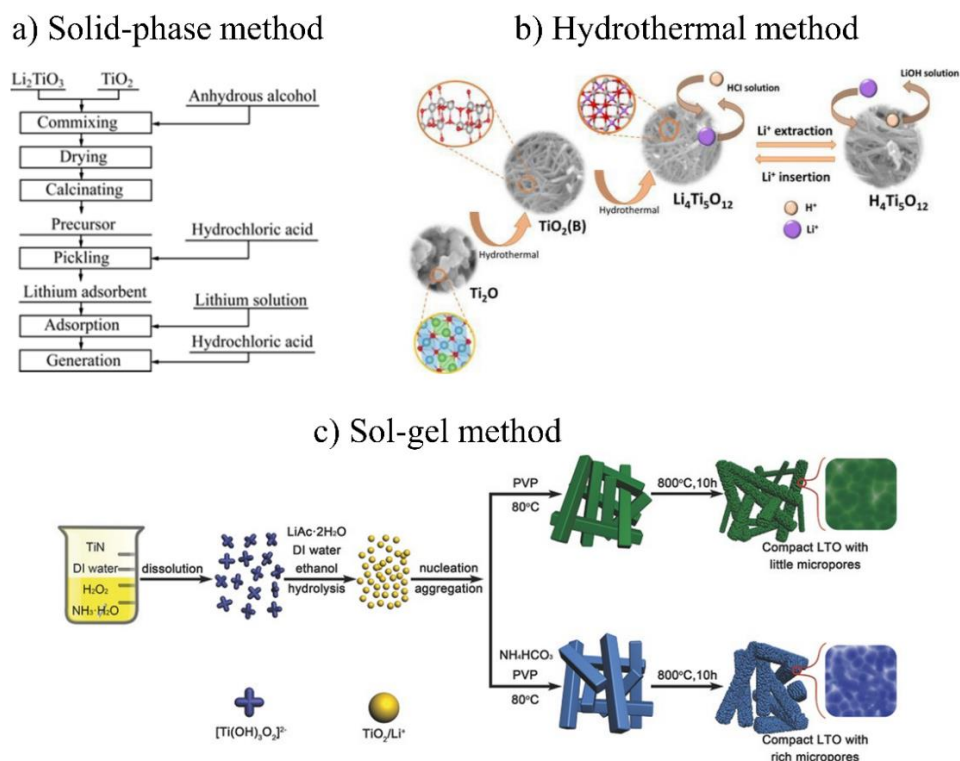
357 The synthesis strategies of LTO adsorbent highlight solid-phase [161, 164], sol-gel [170], and
 358 hydrothermal methods [171, 172] for precursor preparation (concluded in **Table 3** and **Fig. 8**) and

359 acid treatment for ion-sieve fabrication. The conventional solid-phase process requires the
360 calcination of the ground mixture of TiO_2 and Li_2CO_3 at around 700°C and then cooling down to
361 room temperature, presenting the merits of high capacity and selectivity for Li uptake and the
362 drawbacks of high reaction temperature and large grain sizes with low Li adsorption rate [164].
363 Shi et al. utilized mixed crystal titanium dioxide (TiO_2) to compound single crystal phase of HTO
364 through the solid-phase and hydrochloric solution immersing methods [161]. Hossain et al.
365 prepared HTO from sludge-generated TiO_2 via 4-h calcination in air at 750°C , and the Ti loss was
366 less than 3% after 72-h acid treatment [173]. Gu et al. applied the Li adsorbent derived via the
367 solid-state method from $\text{C}_2\text{H}_3\text{LiO}_2 \cdot 2\text{H}_2\text{O}$ and TiO_2 to separate Li and Mg in West Taijinar Lake.
368 The separation factor α (Li/Mg) of 5441.17 and the adsorption capacity of 24.5 mg/g after five
369 cycles demonstrated the feasibility of practical use [174]. Zhang et al. observed that calcination of
370 metatitanic acid produced different crystal phases of TiO_2 at various temperatures and that the
371 anatase structure reacted with $\text{LiOH} \cdot \text{H}_2\text{O}$ benefited the extraction of Li [175]. The sol-gel process
372 produces smaller particle sizes using multiple raw materials at a lower reaction temperature than
373 the solid-phase method. Zhang et al. synthesized Li_2TiO_3 with CH_3COOLi and $\text{Ti}(\text{OC}_4\text{H}_9)_4$ by the
374 sol-gel process, of which the Li adsorption capacity reached 21.0 mg/g [176]. The hydrothermal
375 method, widely utilized in the controllable synthesis of non-agglomerative nanomaterials, is also
376 a typical approach in LTO synthesis. Moazeni et al. synthesized monoclinic $\text{Li}_4\text{Ti}_5\text{O}_{12}$ nanotube
377 ion sieves with 50-70 nm in diameter and 1-2 micrometers in length via a soft hydrothermal
378 method, which presented outstanding Li selective adsorption capacity [171]. Zhao et al. fabricated
379 a $\text{Li}_4\text{Ti}_5\text{O}_{12}$ adsorbent with 5 μm length along the [100] direction by two hydrothermal processes
380 followed by a calcination process and HCl treatment [177]. The $\text{H}_4\text{Ti}_5\text{O}_{12}$ nanotubes synthesized
381 by Shoghi et al. via the hydrothermal method and acid treatment using $\text{TiO}_2(\text{B})$ nanotubes as a

382 precursor demonstrated a considerable high ion-exchange capacity (160.6 mg/g) for Li since the
383 particular surface area was large (115.4 m²/g) [178]. Wang et al. composited a Li-enriched β -
384 Li₂TiO₃ by hydrothermal treatment with the TBA addition. It initially validated the enhancement
385 of the Li adsorption capacity of the free hydrogen formation of β -Li₂TiO₃ and excessive HTi₂ layer
386 exposure of HTO [172]. To overcome the difficulty that the adsorption capacity of LTO-LIS
387 adsorbent is only about 40% of the theoretical value [58], doping strategy was induced in the
388 synthesis process to improve the stability and practical capacity through flexible modification of
389 the band structure of the materials [178, 179]. Wang et al. prepared a Fe-Ti-0.15(H) Li-ion sieve
390 via solid-state reactions and acid treatment and a Mo-Ti-0.15(H) Li-ion sieve with a high O₂-
391 content (61.58%) using a facile calcination method and acid pickling, which showed good stability,
392 capacity and excellent selectivity [180, 181].

393 Composite strategy is also introduced in LTO adsorbent synthesis to produce composite
394 materials [182]. Lawagon et al. selected hydrophilic polyacrylonitrile (PAN) from various
395 polymers as the HTO matrix and fabricated nanofibers (NFs) by electrospun technology. The NFs
396 showed excellent Li selectivity, capacity, durability, recyclability, and suitability for various
397 aqueous Li sources [183]. Lin et al. employed acid-alkali resistant polyvinyl chloride (PVC) as a
398 binder to granulate polyporous PVC-HTO adsorbents, exhibiting high separation factors between
399 Li and Na, K, Ca of 297.55, 521.28, 273.58, respectively, in geothermal brine [184]. Limjuco et
400 al. prepared a HTO/polyvinyl alcohol (PVA) (200 wt% HTO loading) composite foam, which
401 exhibited consistent adsorption-desorption performance and mechanical stability in reusability
402 experiments [185]. Marthi et al. adopted titania slag and diatomaceous earth as raw materials to
403 synthesize HTO-DE composite adsorbent for extracting Li from the Great Salt Lake. They
404 perceived that the Li uptake rate and the adsorption capacity in brine solution were influenced by

405 the competition of ions and the accumulation of protons and that adsorption sites were lost due to
 406 the hydrolysis of metastable HTO at higher temperatures [186]. Zhang et al. coalesced
 407 HTO powders prepared by solid-phase reaction of TiO_2 and Li_2CO_3 in LiCl molten-salt with the
 408 forming agent polyvinyl butyral (PVB), obtaining chemically stable spherical adsorbent particles.
 409 This synthesis method had a lower cost than the traditional solid-phase reaction approach, while
 410 the adsorption capacity and microstructure stability remained, displaying a promising industrial
 411 outlook [187]. Chen et al. developed a novel and easily reused granular and porous Ti-based Li-
 412 ion sieve with the agar-assisted approach for recovering Li from geothermal water [188]. Wei et
 413 al. prepared porous Ti-based nanofiber adsorbents with Li adsorption capacity of 59.1 mg/g and
 414 high selectivity and stability from brine water via a combination strategy of electrospinning and
 415 calcination [189]. Qian et al. prepared a series of HTO/cellulose aerogels with a porous network
 416 for recovering Li from seawater rapidly and efficiently [190].



417
 418 **Figure 8.** Schematic illustration of synthesis of LTO with a) solid-phase method, b) hydrothermal

419 method, and c) sol-gel method. (a) obtained from [161] and (b) from [178] with copyright
420 permission from Elsevier. (c) obtained from [191] (copyright 2017 John Wiley and Sons).

421 For improving the performances of the adsorbents, optimal operation conditions are
422 investigated. Zhu et al. reported that the shaping process did not impact the phase and pore
423 structure of LTO adsorbents, while higher pH was beneficial to strengthening adsorption strength
424 and increasing Li adsorption capacity notably [192]. Li et al. discovered that the adsorption process
425 is mainly single-layer chemical adsorption by modeling the adsorption kinetics process of the LTO
426 adsorbent, prepared by acid elution of a pure monoclinic spinel precursor [193]. Shi et al. found
427 that the Li adsorption process conformed to the Langmuir equation with monolayer adsorption and
428 pseudo-second-order rate model and that the optimal situation should be in the alkaline solution
429 [161]. Lawagon et al. identified the Li adsorption process as endothermic and spontaneous and
430 detected that a low ratio of its loading with the feed volume (i.e., low S/L ratio) could promote the
431 performances of the HTO adsorbent [194]. Ooi et al. calculated the experimental Li elution curves
432 by modeling and proposed conditions of having the eluate of high Li concentration in a short time
433 [195]. Li et al. investigated the influence of the different crystal phases of TiO₂ precursors
434 (amorphous, anatase, and rutile) on the adsorption performances of the terminated LTO and
435 discovered a positive correlation between hydrophilicity and the adsorption performance of HTO
436 based on contact angle experiments [196]. As for the influence of co-existing ions, Ji et al. noticed
437 a slight influence of co-existing metal ions in the aqueous solution on Li recovery when searching
438 the optimal synthesis conditions of their monoclinic crystal HTO [197]. Chitrakar et al. found that
439 the size effect contributed to the HTO efficiently adsorbing Li from the salt lake brine collected
440 from Salar de Uyuni, Bolivia, which contained competitive cations such as sodium, potassium,
441 magnesium, and calcium in considerable excess [164].

442 **Table 3.** Synthesis methods and performances of Ti-based adsorbents

Precursors	Sources	Preparation	Li uptake capacity	Ref.
Li ₂ TiO ₃	TiO ₂ , Li ₂ TiO ₃	Solid-phase method	32.6 mg/g in brine containing NaHCO ₃	[164]
Li ₂ TiO ₃	CH ₃ COOLi, Ti(OC ₄ H ₉) ₄	Sol-gel method	21.0 mg/g after a treatment 24 h	[176]
Li ₂ TiO ₃	TiO ₂ , LiOH·H ₂ O	Hydrothermal method	76.7 mg/g in LiOH solution (2g/L of Li) at 30°C for 24h	[172]
Li ₂ TiO ₃	Titania slag NaOH	Hydrothermal method	27.4 mg/g in LiCl buffered solution(pH=9.5)	[186]
Li ₂ TiO ₃	Li ₂ TiO ₃ , TiO ₂ , ethanol	Liquid-solid phase method	34.2 mg/g in Li-containing solution	[196]
Li ₂ TiO ₃	Ti ₂ (SO ₄) ₃ , LiCOOH, NH ₃ ·H ₂ O, H ₂ O ₂	Precipitation- peptization method	33.35 mg/g within 8h	[198]
Li ₂ TiO ₃	C ₂ H ₃ LiO ₂ ·2H ₂ O, TiO ₂	Liquid-solid phase method	24.5 mg/g after 5 adsorption-desorption cycles	[174]
Li ₂ TiO ₃	TiO ₂ , LiOH·H ₂ O	Solid-phase method	52 mg/g in LiOH solutions (1.8 g/L of Li, pH=12)	[199]
Mo-doped Li ₂ TiO ₃	TiO ₂ , LiOH·H ₂ O, MoO ₂	Solid-phase method	78 mg/g in LiOH solution (1.8g/L of Li at room temperature)	[180]
Fe-doped Li ₂ TiO ₃	TiO ₂ , LiOH·H ₂ O, Fe ₂ O ₃	Solid-phase method	34.8 mg/g in adjusted brine with 1560 mg/L of Li	[200]
Li ₄ Ti ₅ O ₁₂	TiO ₂ , NaOH, LiOH	Two-step hydrothermal method	39.43 mg/g in 120 mg/L of Li solution	[171]
Li ₄ Ti ₅ O ₁₂	TiO ₂ , NaOH, LiOH	Hydrothermal method	160.6 mg/g in the LiCl solution with 2000 mg/L of Li	[178]

443 *2.4 Comparison of three types of metal-based Li adsorbents*

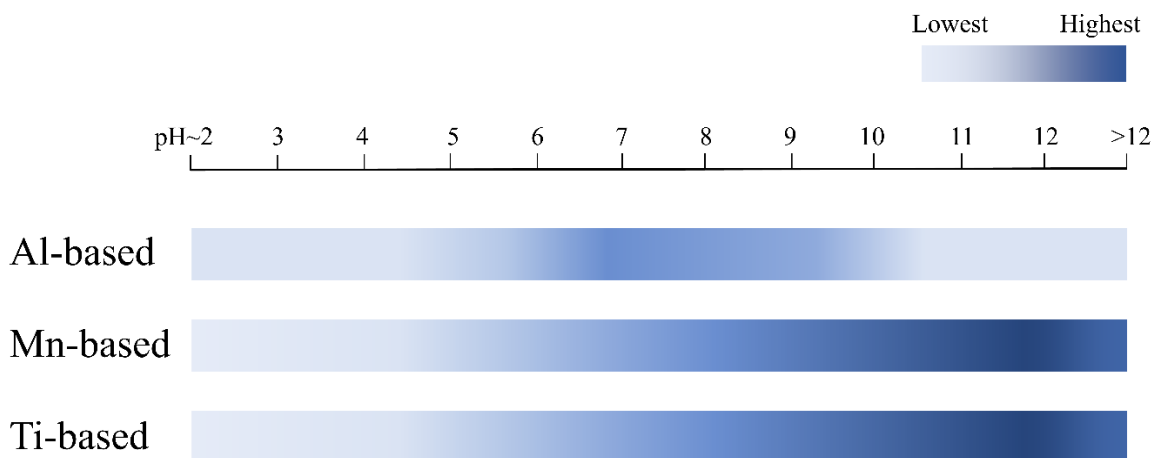
444 **Table 4** compared the Li adsorption capacities, selectivity, technology maturity, stability and
 445 regeneration ability, operation condition requirement, environmental safety, and preparation cost
 446 of three types of metal-based Li adsorbents in their optimal operation conditions. Capacities reflect
 447 the Li adsorption ability; selectivity presents Li adsorption advantages in the competition with
 448 other co-existing ions; technology maturity, stability, regeneration ability, operation condition
 449 requirement, environmental safety, and preparation cost are the most significant factors in
 450 industrial scale-up and commercial applications. Al-based adsorbents have the highest technology
 451 maturity but lowest capacity. Mn-based adsorbents show good selectivity, yet the Mn loss during
 452 desorption can be harmful to the water environment. Ti-based adsorbents present remarkable
 453 capacity, but further investigations on fabrication for scale-up applications are required since the
 454 performances decrease dramatically after granulating the powdery adsorbents.

455 **Table 4.** Comparison of three types of metal-based adsorbents

Performance	Al-based	Mn-based	Ti-based
Li Adsorption Capacity	★☆☆	★★★	★★★
Li Selectivity	★☆☆	★★★	★★★
Technology Maturity	★★★	★★★	★★★
Stability and Regeneration Ability	★★★	★★★	★★★
Facile Operation Condition	★★★	★★★	★★★
Environmental Safety	★★★	★★★	★★★
Low Preparation Cost	★★★	★★★	★★★

456

457 Due to the Li-H ion-exchange adsorption mechanism, pH is a critical condition to influence
 458 the capacities of metal-based Li adsorbents. Al-based adsorbents show the best performance in
 459 neutral solutions, while Mn-based and Ti-based adsorbents have the highest capacities in basic
 460 conditions [94, 141, 144, 192, 201-207]. **Fig. 9** compared the influence of pH on each type of
 461 metal-based Li adsorbents.



462

463 **Figure 9.** The capacity performances of metal-based Li adsorbents under different pH conditions.

3. Case study - Application of metal-based adsorbent for Li recovery in an actual industrial site

The Qarhan Salt Lake located in Qinghai Province is the largest salt lake with the highest Li reserves in China, with an estimated 10.49 million tons of lithium carbonate equivalents (LCE) reserves [208]. **Table 5** lists the ion compositions of the Qarhan Salt Lake brine. The primary interfering ion is Mg, and the Mg/Li ratio is approximately around 365. The current Li mining right of the Qarhan Salt Lake is held by Qinghai Lakelithium Co., LTD and Golmud Zangge Lithium Co., LTD. In 2021, a 20000-tonne-scale plant with adsorption technology was built at Qarhan Salt Lake by Qinghai Lakelithium Co., LTD, and a trial run was successfully completed.

Table 5. Ion Compositions of the Qarhan Salt Lake brine [67]

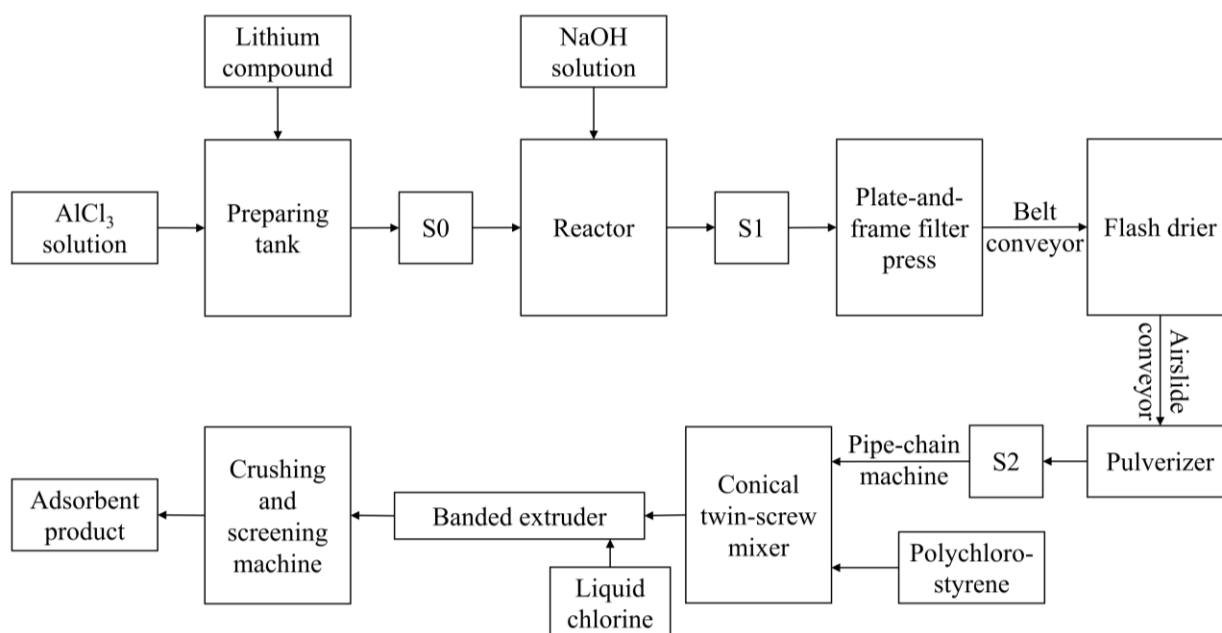
Li	Na	Mg	Ca	B	Cl	SO ₄	Mg/Li
0.35	1.866	127.9	0.04	0.39	334.8	11.6	365.43

3.1 Adsorbent production and regeneration technologies

The production process of the Al-based adsorbent $[\text{LiCl} \cdot (2.2 \sim 2.8)\text{Al}(\text{OH})_3 \cdot (2.7 \sim 3.9)\text{H}_2\text{O}]$ for Li recovery from the Qarhan Salt Lake is shown in **Fig. 10**. Firstly, AlCl_3 solution and Li compound ($\text{LiOH}/\text{Li}_2\text{CO}_3/\text{LiCl}$) are mixed thoroughly in a preparing tank, forming an intermediate product S0. The ratio of Al and Li should be 1.8-2.2:1. For example, 148 g Li_2CO_3 or 2 L LiOH solution (60 g/L) is added in 8 L AlCl_3 solution (120 g/L). Then, S0 and NaOH solution react in a reactor, generating an intermediate product S1. Next, S1 is separated, washed, dried, and ground to powder S2, and S3 is granulated by adding adhesive and liquid chlorine into S2. Finally, S3 is crushed and screened to produce Li adsorbents. The granular size of the final product is 0.5-1.8 mm, and the specific surface area is 2.9 m^2/g . The adsorption equivalent is 1.8-2.7 g/kg, and the loss rate in washing is 12-30% [209].

The adsorption performance of the adsorbent will decrease after the long-term operation in

487 the adsorption chamber because hydroxide precipitates caused by hydrolysis reaction gradually
 488 adhere to the surface of the Li adsorbent and block the inner pores. Thus, a regeneration process
 489 is necessary to reduce adsorbent loss and control the cost. The ammonium salt solution with a
 490 concentration of 0.6-2.0 kg/m³ prepared in the mixing chamber using concentrated ammonium salt
 491 solution and salt-free water is infused into the adsorption chamber to meet with saturated
 492 adsorbents for a residence time (around 3 hours). In this process, during Li desorbing, the
 493 obstruction in adsorbents reacts with ammonium salt and dissolves in solution, and adsorbents
 494 regenerate. Finally, the desorbed LiCl solution and dissolved obstruction flow to the desorption
 495 solution tank [210].

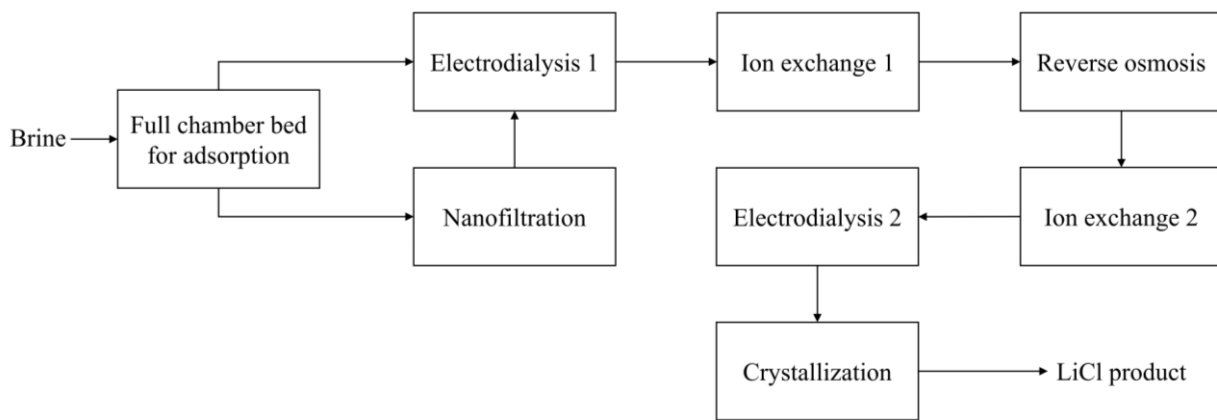


496
 497 **Figure 10.** Flow sheet of adsorbent production. S0, S1, S2 represent intermediate products 1, 2, 3,
 498 respectively.

499 3.2 Li recovery process and operation

500 Li production on a commercial scale typically adopts integrated processes in terms of the
 501 compositions of different brine sources. **Fig. 11** presents the overall process of Li recovery in this

502 case. The path starts from adsorption in a full chamber bed. In specific scenarios, based on the Li
 503 concentration in the desorbed LiCl solution, nanofiltration is sometimes employed prior to
 504 electrodialysis as a pretreatment. Upon electrodialysis pretreatment, the main train of processes
 505 involves, firstly, ion exchange, reverse osmosis, and secondly ion exchange, followed by
 506 electrodialysis, and crystallization, to finally obtain LiCl product with high purity ($\text{LiCl} > 99.1\%$)
 507 [211, 212].



508
 509 **Figure 11.** Li recovery process. Adsorption using a full chamber bed is the first step for
 510 concentrating LiCl solution from the brine.

511 The operation conditions in the adsorption process are listed in **Table 6**. The brine is injected
 512 into the adsorption tower loaded with low-Li-state adsorbents. After an adsorption process, the
 513 adsorbents become adsorbed-state, and the adsorption tail solution is discharged out of the
 514 adsorption unit. Next, the rinse solution is injected into the adsorption tower, and then the rinse
 515 tail solution is discharged out of the adsorption unit. Finally, the desorption solution is injected
 516 into the adsorption tower. After a desorption process, the adsorbents return to a low-Li state, and a
 517 high-Li mother solution is obtained and transferred to the next process unit. The discharged
 518 adsorption tail solution and rinse tail solution are mixed and injected back into the adsorption tower.
 519 The above step is repeated several times to produce concentrated LiCl solution continuously. The

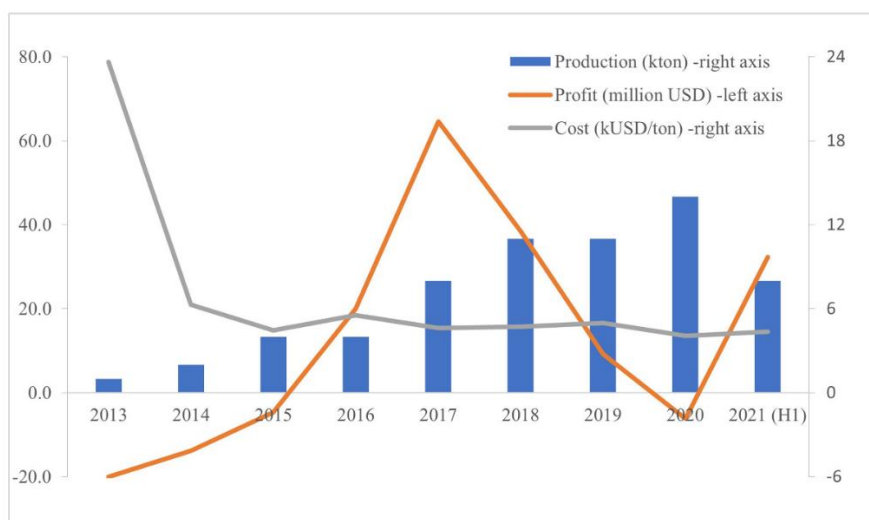
520 desorption tail solution is left in the adsorption tower. The desorbed solution (high-Li mother
 521 solution) comprises of 0.4-0.9 g/L Li, 0.5-8.0 g/L Mg, 0.01-0.2 g/L Na, 2-20 g/L Cl. The recovery
 522 rate of LiCl reaches 40-60% [211-213].

523 **Table 6.** Operation conditions in the adsorption process [211].

Adsorption flow velocity	Adsorption temperature	Rinse flow velocity	Rinse temperature	Desorption flow velocity	Desorption temperature
5-8 m/h	10-25°C	10-20 m/h	10-25°C	10-20 m/h	20-40°C

524 *3.3 Cost, benefit, and economic evaluation*

525 The novel production lines with the adsorption method win the attention of Lakelithium Co.
 526 LTD from the Li market, even stimulating the share price of its parent companies to surge. In the
 527 past years, the Chinese market has shown unprecedented confidence in Li recovery from brines
 528 since new technologies can reduce the cost of production. The unit profits, productions, and costs
 529 of Li carbonate products from 2013 to 2021 are exhibited in **Fig. 12**. According to the financial
 530 reports and market survey reports [214, 215], the current cost of Li recovery can be controlled
 531 within 34000 RMB/ton (around 5340 USD/ton). Compared with membrane and electro dialysis
 532 processes, the overall capital expenditure on adsorption technology is higher. Thus, the future
 533 production expansion can further reduce the unit cost and increase the profit margin.



534
 535 **Figure 12.** The unit profits, productions, and costs of Li₂CO₃ from 2013 to 2021 (data from [208]).

536 The US National Renewable Energy Laboratory investigated seven Li extraction projects
 537 from geothermal brines in various companies to compare Li recovery costs through different
 538 methods. The survey and modeled data of productions, production costs, capital expenses
 539 (CAPEX), operating expenses (OPEX), product prices, and Li recovery are listed in **Table 7**.
 540 Although direct cost comparison of different locations requires a number of assumptions and,
 541 therefore, to some degree, is unfair, the data is able to provide a broad visualization of economic
 542 indicators based on different approaches. The pilot plant project of Vulcan Energy Resources using
 543 commercial adsorbents performs outstandingly with the low production cost and high Li recovery
 544 rate.

545 **Table 7.** Summary of Li recovery project economics. Table obtained from [216] (copyright
 546 National Renewable Energy Laboratory).

Company	Production (mt/y)	Production cost (USD/mt)	CAPEX (kUSD)	OPEX (kUSD/y)	Product price (USD/mt)	Technology	Li recovery rate
SRI International	20000	3845	52300	76900	12000	Li-imprinted polymer	90%
Vulcan Energy Resources	40000	3217	1287600	128688	14925	Commercial adsorbents	90%
Standard Lithium	20900	4319	437162	90259	13550	Ceramic adsorbent and crystallization	90%
E3 Metals Corp	20000	3656	602000	73200	15160	Ion exchange	>90%
Anson Resources	15000	4545	120000	68180	13000	Ion exchange	75%
Pure Energy Minerals	11500	3217	358601	36516	12267	Solvent extraction	90%
Lake Resources	25500	4178	544000	106539	11000	Ion exchange	83.2%

547 **4. Outlook and Conclusions**

548 Li extraction from aqueous resources by Al, Mn, and Ti-based metal adsorbents, is
 549 comprehensively reviewed in terms of synthesis methods, Li uptake mechanisms, and Li recovery
 550 performances. Al-based adsorbents have been employed as commercial adsorbents in the industry
 551 due to the relatively mature preparation technology, low-cost price, and stability, although their Li
 552 adsorption capacity is lower than Mn-based and Ti-based adsorbents. A number of different types

553 of Mn-based adsorbents can be developed based on Li/Mn ratio in precursors, and the formations
554 of the crystals rely on the control of synthesis conditions. Although Mn-based adsorbents present
555 promising potential in Li adsorption capacity, the Mn loss problem still prevents further scale-up
556 applications, requiring more investigations on stability improvements such as doping and coating.
557 Ti-based adsorbents exhibit good stability in acidic surroundings with low leaching issues, yet
558 practical adsorption capacity is inferior to theoretical capacity. Besides, an industrial case study is
559 introduced to analyze the operation process and economic behavior, giving an example and
560 benchmark for the application developments for commercial adsorbents.

561 The substantial Li demand promotes the rapid transition of lab-state research to engineering
562 projects. Overall, the adsorbent productions and Li recovery processes show advantages of simple
563 operation, high maturity, and strong reliability. The metal-based adsorbent presents good Li
564 selectivity, high adsorption efficiency, and environmental-friendly property. Nevertheless, major
565 limitations such as poor versatility, low reuse frequency, and dissolution loss hinder industrial
566 applications. Scaling up to a large-scale plant is the ultimate goal for all kinds of adsorbents.
567 Therefore, the study on metal-based adsorbents in Li recovery should be focused on 1) stability
568 improvement to achieve the long-term operation goal, 2) adsorbent explorations for different
569 application conditions, such as resources with different pH, Li contents, and temperatures, 3)
570 economical process design to reduce operating cost, 4) hybrid process optimization to produce
571 valuable net-worth products with high Li purity.

572

573 **Declaration of competing interest**

574 The authors declare that they have no known competing financial interests or personal
575 relationships that could have appeared to influence the work reported in this paper.

576 Acknowledgment

577 We thank financial support from the Qatar National Research Fund under its National
578 Priorities Research Program (NPRP 12S-0227-190166), Australian Research Council (ARC,
579 IH210100001), Australian Indian Strategic Research Funding (Round 12 AIRXII000019), and
580 Australian Research Council Discovery Early Career Research Award (DE200100661).

581

582 References

- 583 1. Choubey, P.K., et al., *Advance review on the exploitation of the prominent energy-storage*
584 *element: Lithium. Part I: From mineral and brine resources*. Minerals Engineering, 2016. **89**: p.
585 119-137.
- 586 2. Martin, G., et al., *Lithium market research – global supply, future demand and price*
587 *development*. Energy Storage Materials, 2017. **6**: p. 171-179.
- 588 3. USGS, *Mineral Commodity Summaries 2021*, in *Mineral Commodity Summaries*. 2021.
- 589 4. USGS, *Mineral Commodity Summaries 2022*, in *Mineral Commodity Summaries*. 2022.
- 590 5. USGS, *Mineral Commodity Summaries 2021*. 2021.
- 591 6. USGS, *Mineral Commodity Summaries 2020*, in *Mineral Commodity Summaries*. 2020.
- 592 7. USGS, *Mineral Commodity Summaries 2019*, in *Mineral Commodity Summaries*. 2019.
- 593 8. Hou, J., et al., *Lithium Extraction by Emerging Metal-Organic Framework-Based Membranes*.
594 *Advanced Functional Materials*, 2021. **31**(2105991).
- 595 9. Yang, S., et al., *Lithium Metal Extraction from Seawater*. Joule, 2018. **2**(9): p. 1648-1651.
- 596 10. Vikström, H., S. Davidsson, and M. Höök, *Lithium availability and future production outlooks*.
597 *Applied Energy*, 2013. **110**: p. 252-266.
- 598 11. Grosjean, C., et al., *Assessment of world lithium resources and consequences of their geographic*
599 *distribution on the expected development of the electric vehicle industry*. Renewable and
600 *Sustainable Energy Reviews*, 2012. **16**(3): p. 1735-1744.
- 601 12. Swain, B., *Recovery and recycling of lithium: A review*. Separation and Purification Technology,
602 2017. **172**: p. 388-403.
- 603 13. Zhang, Y., et al., *Systematic review of lithium extraction from salt-lake brines via precipitation*
604 *approaches*. Minerals Engineering, 2019. **139**(105868).
- 605 14. Li, X., et al., *Membrane-based technologies for lithium recovery from water lithium resources: A*
606 *review*. Journal of Membrane Science, 2019. **591**(117317).
- 607 15. Coterillo, R., et al., *Selective extraction of lithium from seawater desalination concentrates: Study*
608 *of thermodynamic and equilibrium properties using Density Functional Theory (DFT)*.
609 *Desalination*, 2022. **532**(115704).
- 610 16. Shi, D., et al., *Removal of calcium and magnesium from lithium concentrated solution by solvent*
611 *extraction method using D2EHPA*. Desalination, 2020. **479**(114306).
- 612 17. Jiang, H., et al., *Synergic and competitive adsorption of Li-Na-MgCl₂ onto lithium-aluminum*
613 *hydroxides*. Adsorption, 2020. **26**(7): p. 1039-1049.
- 614 18. Battistel, A., et al., *Electrochemical Methods for Lithium Recovery: A Comprehensive and*
615 *Critical Review*. Adv Mater, 2020. **32**(1905440).
- 616 19. Liu, D., et al., *A closed-loop process for selective lithium recovery from brines via*
617 *electrochemical and precipitation*. Desalination, 2021. **519**(115302).

- 618 20. Palagonia, M.S., D. Brogioli, and F. La Mantia, *Lithium recovery from diluted brine by means of*
619 *electrochemical ion exchange in a flow-through-electrodes cell*. Desalination, 2020.
620 **475**(114192).
- 621 21. Bazrgar Bajestani, M., A. Moheb, and M. Dinari, *Preparation of lithium ion-selective cation*
622 *exchange membrane for lithium recovery from sodium contaminated lithium bromide solution by*
623 *electrodialysis process*. Desalination, 2020. **486**(114476).
- 624 22. Perez-Antolin, D., et al., *Regenerative electrochemical ion pumping cell based on semi-solid*
625 *electrodes for sustainable Li recovery*. Desalination, 2022. **533**(115764).
- 626 23. Xu, Y., et al., *High performance Mg²⁺/Li⁺ separation membranes modified by a bis-quaternary*
627 *ammonium salt*. Desalination, 2022. **526**(115519).
- 628 24. He, R., et al., *Unprecedented Mg²⁺/Li⁺ separation using layer-by-layer based nanofiltration*
629 *hollow fiber membranes*. Desalination, 2022. **525**(115492).
- 630 25. Zhang, C., et al., *Lithium extraction from synthetic brine with high Mg²⁺/Li⁺ ratio using the*
631 *polymer inclusion membrane*. Desalination, 2020. **496**(114710).
- 632 26. İpekçi, D., et al., *Application of heterogeneous ion exchange membranes for simultaneous*
633 *separation and recovery of lithium and boron from aqueous solution with bipolar membrane*
634 *electrodialysis (EDBM)*. Desalination, 2020. **479**(114313).
- 635 27. Paredes, C. and E. Rodríguez de San Miguel, *Selective lithium extraction and concentration from*
636 *diluted alkaline aqueous media by a polymer inclusion membrane and application to seawater*.
637 Desalination, 2020. **487**(114500).
- 638 28. Guo, X., et al., *Highly Efficient Separation of Magnesium and Lithium and High-Valued*
639 *Utilization of Magnesium from Salt Lake Brine by a Reaction-Coupled Separation Technology*.
640 Industrial & Engineering Chemistry Research, 2018. **57**(19): p. 6618-6626.
- 641 29. Sun, Y., et al., *Recent advances in magnesium/lithium separation and lithium extraction*
642 *technologies from salt lake brine*. Separation and Purification Technology, 2021. **256**(117807).
- 643 30. Khalil, A., et al., *Lithium recovery from brine: Recent developments and challenges*.
644 Desalination, 2022. **528**(115611).
- 645 31. Zhao, Y., et al., *An integrated membrane process for preparation of lithium hydroxide from high*
646 *Mg/Li ratio salt lake brine*. Desalination, 2020. **493**(114620).
- 647 32. Ying, J., et al., *Selective separation of lithium from high Mg/Li ratio brine using single-stage and*
648 *multi-stage selective electrodialysis processes*. Desalination, 2020. **492**(114621).
- 649 33. Flexer, V., C.F. Baspineiro, and C.I. Galli, *Lithium recovery from brines: A vital raw material for*
650 *green energies with a potential environmental impact in its mining and processing*. Sci Total
651 Environ, 2018. **639**: p. 1188-1204.
- 652 34. An, J.W., et al., *Recovery of lithium from Uyuni salar brine*. Hydrometallurgy, 2012. **117-118**: p.
653 64-70.
- 654 35. Kenta Onishi, T.N., Syouhei Nishihama, and Kazuharu Yoshizuka, *Synergistic Solvent*
655 *Impregnated Resin for Adsorptive Separation of Lithium Ion*. Industrial & Engineering Chemistry
656 Research, 2010. **49**(14): p. 6554-6558.
- 657 36. Masmoudi, A., et al., *Solvent extraction of lithium ions using benzoyltrifluoroacetone in new*
658 *solvents*. Separation and Purification Technology, 2021. **255**(117653).
- 659 37. Hong, Z., et al., *Dependence of concentration polarization on discharge profile in*
660 *electrochemical lithium extraction*. Desalination, 2022. **527**(115567).
- 661 38. M. Bryjak, A.S., J. Kujawski, K. Smolinska-Kempisty, W. Kujawski, *Capacitive deionization for*
662 *selective extraction of lithium from aqueous solutions*. Journal of Membrane and Separation
663 Technology, 2015. **4**: p. 110-115.
- 664 39. Sahin, S., et al., *Enhanced monovalent over divalent cation selectivity with polyelectrolyte*
665 *multilayers in membrane capacitive deionization via optimization of operational conditions*.
666 Desalination, 2022. **522**(115391).
- 667 40. Chen, Z., et al., *Ultra-durable and highly-efficient hybrid capacitive deionization by MXene*
668 *confined MoS₂ heterostructure*. Desalination, 2022. **528**(115616).

- 669 41. Zavahir, S., et al., *A review on lithium recovery using electrochemical capturing systems*.
670 Desalination, 2021. **500**(114883).
- 671 42. Zhao, W.-Y., et al., *Waste Conversion and Resource Recovery from Wastewater by Ion Exchange*
672 *Membranes: State-of-the-Art and Perspective*. Industrial & Engineering Chemistry Research,
673 2018. **57**(18): p. 6025-6039.
- 674 43. Liu, G., Z. Zhao, and L. He, *Highly selective lithium recovery from high Mg/Li ratio brines*.
675 Desalination, 2020. **474**(114185).
- 676 44. Sharma, P.P., et al., *Sulfonated poly (ether ether ketone) composite cation exchange membrane*
677 *for selective recovery of lithium by electrodialysis*. Desalination, 2020. **496**(114755).
- 678 45. Siekierka, A., *Lithium and magnesium separation from brines by hybrid capacitive deionization*.
679 Desalination, 2022. **527**(115569).
- 680 46. Siekierka, A. and M. Bryjak, *Selective sorbents for recovery of lithium ions by hybrid capacitive*
681 *deionization*. Desalination, 2021. **520**(115324).
- 682 47. Siekierka, A., *Lithium iron manganese oxide as an adsorbent for capturing lithium ions in hybrid*
683 *capacitive deionization with different electrical modes*. Separation and Purification Technology,
684 2020. **236**(116234).
- 685 48. Gong, L., et al., *Direct numerical simulation of continuous lithium extraction from high Mg²⁺/Li⁺*
686 *ratio brines using microfluidic channels with ion concentration polarization*. J Memb Sci, 2018.
687 **556**: p. 34-41.
- 688 49. Limjoco, L.A., et al., *Aerosol Cross-Linked Crown Ether Diols Melded with Poly(vinyl alcohol)*
689 *as Specialized Microfibrous Li⁺ Adsorbents*. ACS Appl Mater Interfaces, 2017. **9**(49): p. 42862-
690 42874.
- 691 50. Liu, W., et al., *Extraction of lithium ions from acidic solution using electrochemically imprinted*
692 *membrane*. Desalination, 2020. **496**(114751).
- 693 51. Pramanik, B.K., et al., *A critical review of membrane crystallization for the purification of water*
694 *and recovery of minerals*. Reviews in Environmental Science and Bio/Technology, 2016. **15**(3):
695 p. 411-439.
- 696 52. Roobavannan, S., S. Vigneswaran, and G. Naidu, *Enhancing the performance of membrane*
697 *distillation and ion-exchange manganese oxide for recovery of water and lithium from seawater*.
698 Chemical Engineering Journal, 2020. **396**(125386).
- 699 53. Ryu, T., et al., *Recovery of Lithium by an Electrostatic Field-Assisted Desorption Process*.
700 Industrial & Engineering Chemistry Research, 2013. **52**(38): p. 13738-13742.
- 701 54. Choi, J., H. Lee, and S. Hong, *Capacitive deionization (CDI) integrated with monovalent cation*
702 *selective membrane for producing divalent cation-rich solution*. Desalination, 2016. **400**: p. 38-
703 46.
- 704 55. Shi, W., et al., *Efficient lithium extraction by membrane capacitive deionization incorporated*
705 *with monovalent selective cation exchange membrane*. Separation and Purification Technology,
706 2019. **210**: p. 885-890.
- 707 56. Zhang, Y., et al., *Selectrodialysis: Fractionation of divalent ions from monovalent ions in a novel*
708 *electrodialysis stack*. Separation and Purification Technology, 2012. **88**: p. 191-201.
- 709 57. Ge, L., et al., *Electrodialysis with nanofiltration membrane (EDNF) for high-efficiency cations*
710 *fractionation*. Journal of Membrane Science, 2016. **498**: p. 192-200.
- 711 58. Luo, Q., et al., *Extraction of lithium from salt lake brines by granulated adsorbents*. Colloids and
712 Surfaces A: Physicochemical and Engineering Aspects, 2021. **628**(127256).
- 713 59. Orooji, Y., et al., *Recent advances in nanomaterial development for lithium ion-sieving*
714 *technologies*. Desalination, 2022. **529**(115624).
- 715 60. Xu, P., et al., *Materials for lithium recovery from salt lake brine*. Journal of Materials Science,
716 2020. **56**(1): p. 16-63.
- 717 61. Xu, X., et al., *Extraction of lithium with functionalized lithium ion-sieves*. Progress in Materials
718 Science, 2016. **84**: p. 276-313.

- 719 62. Weng, D., et al., *Introduction of manganese based lithium-ion Sieve-A review*. Progress in
720 Natural Science-Materials International, 2020. **30**(2): p. 139-152.
- 721 63. Zhao, X., et al., *Review on the electrochemical extraction of lithium from seawater/brine*. Journal
722 of Electroanalytical Chemistry, 2019. **850**(113389).
- 723 64. Zhang, X., A. Han, and Y. Yang, *Review on the production of high-purity lithium metal*. Journal
724 of Materials Chemistry A, 2020. **8**(43): p. 22455-22466.
- 725 65. Meshram, P., B.D. Pandey, and T.R. Mankhand, *Extraction of lithium from primary and
726 secondary sources by pre-treatment, leaching and separation: A comprehensive review*.
727 Hydrometallurgy, 2014. **150**: p. 192-208.
- 728 66. Liu, G., Z. Zhao, and A. Ghahreman, *Novel approaches for lithium extraction from salt-lake
729 brines: A review*. Hydrometallurgy, 2019. **187**: p. 81-100.
- 730 67. Shanshan Xu, J.S., Qiuyan Bi, Qing Chen, Wei-Ming Zhang, Zexin Qian, Lei Zhang, Shiai Xu,
731 Na Tang, Tao He, *Extraction of lithium from Chinese salt-lake brines by membranes: Design and
732 practice*. Journal of Membrane Science, 2021. **635**(119441).
- 733 68. Taghvaie Nakhjiri, A., et al., *Recovery of precious metals from industrial wastewater towards
734 resource recovery and environmental sustainability: A critical review*. Desalination, 2022.
735 **527**(115510).
- 736 69. Ogunbiyi, O., et al., *Sustainable brine management from the perspectives of water, energy and
737 mineral recovery: A comprehensive review*. Desalination, 2021. **513**(115055).
- 738 70. Goh, K.-H., T.-T. Lim, and Z. Dong, *Application of layered double hydroxides for removal of
739 oxyanions: A review*. Water Research, 2008. **42**(6-7): p. 1343-1368.
- 740 71. Chen, J., S. Lin, and J. Yu, *High-selective cyclic adsorption and magnetic recovery performance
741 of magnetic lithium-aluminum layered double hydroxides (MLDHs) in extracting Li⁺ from
742 ultrahigh Mg/Li ratio brines*. Separation and Purification Technology, 2021. **255**(117710).
- 743 72. Kotsupalo, N.P., et al., *Effect of structure on the sorption properties of chlorine-containing form
744 of double aluminum lithium hydroxide*. Russian Journal of Applied Chemistry, 2013. **86**(4): p.
745 482-487.
- 746 73. Zhong, J., S. Lin, and J. Yu, *Li⁺ adsorption performance and mechanism using lithium/aluminum
747 layered double hydroxides in low grade brines*. Desalination, 2021. **505**(114983).
- 748 74. S. G. Kozlova, S.P.G., V. P. Isupov & L.É. Chupakhina, *Using NMR in Structural Studies of
749 Aluminum Hydroxide Intercalation Compounds with Lithium Salts*. Journal of Structural
750 Chemistry, 2003. **44**(2): p. 198–205.
- 751 75. Hou, X.-J., et al., *Structural and electronic analysis of Li/Al layered double hydroxides and their
752 adsorption for CO₂*. Applied Surface Science, 2017. **416**: p. 411-423.
- 753 76. Britto, S. and P.V. Kamath, *Structure of bayerite-based lithium-aluminum layered double
754 hydroxides (LDHs): observation of monoclinic symmetry*. Inorg Chem, 2009. **48**(24): p. 11646-
755 54.
- 756 77. Graham, T.R., et al., *Unraveling Gibbsite Transformation Pathways into LiAl-LDH in
757 Concentrated Lithium Hydroxide*. Inorganic Chemistry, 2019. **58**(18): p. 12385-12394.
- 758 78. Sun, Y., et al., *Highly Efficient Lithium Recovery from Pre-Synthesized Chlorine-Ion-Intercalated
759 LiAl-Layered Double Hydroxides via a Mild Solution Chemistry Process*. Materials (Basel), 2019.
760 **12**(1968).
- 761 79. M Frenkel, A.G., S Sarig, *Crystal Modification of Freshly Precipitated Aluminum Hydroxide by
762 Lithium Ion*. The Journal of Physical Chemistry, 1980. **84**: p. 507-510.
- 763 80. K. R. Poepelmeier, S.-J.H., *Synthesis of Lithium Dialuminate by Salt Imbibition*. Inorganic
764 Chemistry, 1987. **26**: p. 3297-3302.
- 765 81. Qu, J., et al., *Synthesis of Li–Al layered double hydroxides via a mechanochemical route*. Applied
766 Clay Science, 2016. **120**: p. 24-27.
- 767 82. Qu, J., et al., *Mechanochemical approaches to synthesize layered double hydroxides: a review*.
768 Applied Clay Science, 2016. **119**: p. 185-192.

- 769 83. Stepanova, L.N., et al., *The study of structural, textural and basic properties of MgAl- and LiAl-*
770 *LDH prepared by mechanochemical method*. *Catalysis Today*, 2020. **357**: p. 638-645.
- 771 84. Isupov, V.P., et al., *Aluminium hydroxide as selective sorbent of lithium salts from brines and*
772 *technical solutions*. *Adsorption and Its Applications in Industry and Environmental Protection*,
773 *Vol I: Applications in Industry*, 1998. **120**: p. 621-652.
- 774 85. Xuheng Liua, M.Z., Xingyu Chena,b, Zhongwei Zhao, *Separating lithium and magnesium in*
775 *brine by aluminum-based materials*. *Hydrometallurgy*, 2018. **176**: p. 73-77.
- 776 86. Zhong, J., S. Lin, and J. Yu, *Lithium recovery from ultrahigh Mg²⁺/Li⁺ ratio brine using a novel*
777 *granulated Li/Al-LDHs adsorbent*. *Separation and Purification Technology*, 2021. **256**(117780).
- 778 87. Lee, Y., J.H. Cha, and D.Y. Jung, *Selective Lithium Adsorption of Silicon Oxide Coated Lithium*
779 *Aluminum Layered Double Hydroxide Nanocrystals and Their Regeneration*. *Chem Asian J*,
780 2021. **16**(8): p. 974-980.
- 781 88. Sun, Y., et al., *Highly efficient extraction of lithium from salt lake brine by LiAl-layered double*
782 *hydroxides as lithium-ion-selective capturing material*. *Journal of Energy Chemistry*, 2019. **34**: p.
783 80-87.
- 784 89. Lee, Y., J.-H. Cha, and D.-Y. Jung, *Lithium separation by growth of lithium aluminum layered*
785 *double hydroxides on aluminum metal substrates*. *Solid State Sciences*, 2020. **110**(106488).
- 786 90. Lee, Y. and D.-Y. Jung, *Polyacrylonitrile hybrid membrane coated with aluminum hydroxide for*
787 *separating lithium*. *Journal of Physics and Chemistry of Solids*, 2022. **162**(110509).
- 788 91. Jiang, H., Y. Yang, and J. Yu, *Application of concentration-dependent HSDM to the lithium*
789 *adsorption from brine in fixed bed columns*. *Separation and Purification Technology*, 2020.
790 **241**(116682).
- 791 92. Jiang, H., et al., *Adsorption of lithium ions on lithium-aluminum hydroxides: Equilibrium and*
792 *kinetics*. *The Canadian Journal of Chemical Engineering*, 2019. **98**(2): p. 544-555.
- 793 93. Zhong, J., S. Lin, and J. Yu, *Effects of excessive lithium deintercalation on Li(+) adsorption*
794 *performance and structural stability of lithium/aluminum layered double hydroxides*. *J Colloid*
795 *Interface Sci*, 2020. **572**: p. 107-113.
- 796 94. Paranthaman, M.P., et al., *Recovery of Lithium from Geothermal Brine with Lithium-Aluminum*
797 *Layered Double Hydroxide Chloride Sorbents*. *Environmental Science & Technology*, 2017.
798 **51**(22).
- 799 95. Hu, F.P., et al., *Quantitative Effects of Desorption Intensity on Structural Stability and*
800 *Readsorption Performance of Lithium/Aluminum Layered Double Hydroxides in Cyclic Li⁺*
801 *Extraction from Brines with Ultrahigh Mg/Li Ratio*. *Industrial & Engineering Chemistry*
802 *Research*, 2020. **59**(30): p. 13539-13548.
- 803 96. Huang, T.-Y., et al., *Life Cycle Assessment and Techno-Economic Assessment of Lithium*
804 *Recovery from Geothermal Brine*. *ACS Sustainable Chemistry & Engineering*, 2021. **9**(19): p.
805 6551-6560.
- 806 97. Wu, L.L., et al., *Lithium aluminum-layered double hydroxide chlorides (LDH): Formation*
807 *enthalpies and energetics for lithium ion capture*. *Journal of the American Ceramic Society*,
808 2019. **102**(5): p. 2398-2404.
- 809 98. Mak Yu, T., et al., *Exploring the surface reactivity of the magnetic layered double hydroxide*
810 *lithium-aluminum: An alternative material for sorption and catalytic purposes*. *Applied Surface*
811 *Science*, 2019. **467-468**: p. 1195-1203.
- 812 99. Chen, J., S. Lin, and J. Yu, *Quantitative effects of Fe₃O₄ nanoparticle content on Li⁺ adsorption*
813 *and magnetic recovery performances of magnetic lithium-aluminum layered double hydroxides in*
814 *ultrahigh Mg/Li ratio brines*. *J Hazard Mater*, 2020. **388**(122101).
- 815 100. Pauwels, H., M. Brach, and C. Fouillac, *Study of Li⁺ adsorption onto polymeric aluminium (III)*
816 *hydroxide for application in the treatment of geothermal waters*. *Colloids and Surfaces A:*
817 *Physicochemical and Engineering Aspects*, 1995. **100**: p. 73-82.
- 818 101. Wang, H., et al., *Recovery of both magnesium and lithium from high Mg/Li ratio brines using a*
819 *novel process*. *Hydrometallurgy*, 2018. **175**: p. 102-108.

- 820 102. Heidari, N. and P. Momeni, *Selective adsorption of lithium ions from Urmia Lake onto aluminum*
821 *hydroxide*. Environmental Earth Sciences, 2017. **76**(16).
- 822 103. Hawash, S., E.A. El Kader, and G. El Diwani, *Methodology for selective adsorption of lithium*
823 *ions onto polymeric aluminium (III) hydroxide*. Journal of American Science, 2010. **6**(11): p. 301-
824 309.
- 825 104. Menzheres, L.T., A.D. Ryabtsev, and E.V. Mamylova, *Synthesis of Selective Sorbent*
826 *LiCl·2Al(OH)₃·nH₂O*. Theoretical Foundations of Chemical Engineering, 2019. **53**(5): p. 821-826.
- 827 105. Liu, D.-F., S.-Y. Sun, and J.-G. Yu, *A new high-efficiency process for Li⁺ recovery from solutions*
828 *based on LiMn₂O₄/λ-MnO₂ materials*. Chemical Engineering Journal, 2019. **377**(119825).
- 829 106. Sun, S.Y., et al., *Lithium extraction/insertion process on cubic Li-Mn-O precursors with different*
830 *Li/Mn ratio and morphology*. Adsorption-Journal of the International Adsorption Society, 2011.
831 **17**(5): p. 881-887.
- 832 107. Zhang, Q.-H., et al., *Lithium selective adsorption on 1-D MnO₂ nanostructure ion-sieve*.
833 *Advanced Powder Technology*, 2009. **20**(5): p. 432-437.
- 834 108. Xiao, J.-L., et al., *Synthesis and Adsorption Properties of Li_{1.6}Mn_{1.6}O₄ Spinel*. Industrial &
835 *Engineering Chemistry Research*, 2013. **52**(34): p. 11967-11973.
- 836 109. Kazunari Yamaura, Q.H., Lianqi Zhang, Kazunori Takada, Yuji Baba, Takuro Nagai, Yoshio
837 Matsui, Kosuke Kosuda, and Eiji Takayama-Muromachi, *Spinel-to-CaFe₂O₄-Type Structural*
838 *Transformation in LiMn₂O₄ under High Pressure*. Journal of the American Chemical Society,
839 2006. **128**(29): p. 9448-9456.
- 840 110. Darul, J., W. Nowicki, and P. Piszora, *Unusual Compressional Behavior of Lithium–Manganese*
841 *Oxides: A Case Study of Li₄Mn₅O₁₂*. The Journal of Physical Chemistry C, 2012. **116**(33): p.
842 17872-17879.
- 843 111. Toshimi Takada, E.A., *Structure Refinement of Li₄Mn₅O₁₂ with Neutron and X-Ray Powder*
844 *Diffraction Data*. Journal of Solid State Chemistry, 1997. **130**: p. 74-80.
- 845 112. Xiao, W., et al., *Insight into fast Li diffusion in Li-excess spinel lithium manganese oxide*. Journal
846 *of Materials Chemistry A*, 2018. **6**(21): p. 9893-9898.
- 847 113. HUNTER, J.C., *Preparation of a new crystal form of manganese dioxide λ-MnO₂*. Journal of
848 *Solid State Chemistry*, 1981. **39**: p. 142-147.
- 849 114. Xiang-MuShen, A., *Phase transitions and ion exchange behavior of electrolytically prepared*
850 *manganese dioxide*. Journal of Solid State Chemistry, 1986. **64**(3): p. 270-282.
- 851 115. Koyanaka, H., et al., *Quantitative correlation between Li absorption and H content in manganese*
852 *oxide spinel λ-MnO₂*. Journal of Electroanalytical Chemistry, 2003. **559**: p. 77-81.
- 853 116. Kenta Ooi, Y.M., Jitsuo Sakakihara, *Mechanism of Li⁺ Insertion in Spinel-Type Manganese*
854 *Oxide. Redox and Ion-Exchange Reactions*. Langmuir, 1991. **7**(6): p. 1167-1171.
- 855 117. Qi Feng, Y.M., Hirofumi Kanoh, and Kenta Ooi, *Li⁺ Extraction/insertion with Spinel-Type*
856 *Lithium Manganese Oxides. Characterization of Redox-Type and Ion-Exchange-Type Sites*.
857 *Langmuir*, 1992. **8**(7): p. 1861-1867.
- 858 118. Yang, X., et al., *Synthesis of Li_{1.33}Mn_{1.67}O₄ spinels with different morphologies and their ion*
859 *adsorptivities after delithiation*. Journal of Materials Chemistry, 2000. **10**(8): p. 1903-1909.
- 860 119. Sun, S.Y., et al., *Synthesis and Adsorption Properties of Li_{1.6}Mn_{1.6}O₄ by a Combination of Redox*
861 *Precipitation and Solid-Phase Reaction*. Industrial & Engineering Chemistry Research, 2014.
862 **53**(40): p. 15517-15521.
- 863 120. N.V. Kosova, N.F.U., E.T. Devyatkina, E.G. Avvakumov, *Mechanochemical synthesis of*
864 *LiMn₂O₄ cathode material for lithium batteries*. Solid State Ionics, 2000. **135**: p. 107-114.
- 865 121. Cui, T., et al., *Preparation and electrochemical properties of LiMn₂O₄ by a rheological-phase-*
866 *assisted microwave synthesis method*. Inorganic Materials, 2008. **44**(5): p. 542-548.
- 867 122. Chu, H.Y., et al., *Study of electrochemical properties and the charge/discharge mechanism for*
868 *Li₄Mn₅O₁₂/MnO₂-AC hybrid supercapacitor*. Journal of Applied Electrochemistry, 2009. **39**(10):
869 p. 2007-2013.

- 870 123. Yang-Kook Sun, I.-H.O., and Kwang Yul Kim, *Synthesis of Spinel LiMn_2O_4 by the Sol-Gel*
871 *Method for a Cathode-Active Material in Lithium Secondary Batteries*. Industrial & Engineering
872 Chemistry Research, 1997. **36**(11): p. 4839-4846.
- 873 124. Thanh, N.T., N. Maclean, and S. Mahiddine, *Mechanisms of nucleation and growth of*
874 *nanoparticles in solution*. Chem Rev, 2014. **114**(15): p. 7610-7630.
- 875 125. YongCai Zhang, H.W., Bo Wang, Hui Yan, Anwar Ahniyaz, Masahiro Yoshimura, *Low*
876 *temperature synthesis of nanocrystalline $\text{Li}_4\text{Mn}_5\text{O}_{12}$ by a hydrothermal method*. Materials
877 Research Bulletin, 2002. **37**(8): p. 1411-1417.
- 878 126. Ramesh Chitrakar, H.K., Yoshitaka Miyai, and Kenta Ooi, *A New Type of Manganese Oxide*
879 *($\text{MnO}_2 \cdot 0.5\text{H}_2\text{O}$) Derived from $\text{Li}_{1.6}\text{Mn}_{1.6}\text{O}_4$ and Its Lithium Ion-Sieve Properties*. Chemistry of
880 Materials, 2000. **12**(10): p. 3151-3157.
- 881 127. Chitrakar, R., et al., *Synthesis of o-LiMnO_2 by Microwave Irradiation and Study Its Heat*
882 *Treatment and Lithium Exchange*. Journal of Solid State Chemistry, 2002. **163**(1): p. 1-4.
- 883 128. Chitrakar, R., et al., *Recovery of lithium from seawater using manganese oxide adsorbent*
884 *($\text{H}_{1.6}\text{Mn}_{1.6}\text{O}_4$) derived from $\text{Li}_{1.6}\text{Mn}_{1.6}\text{O}_4$* . Industrial & Engineering Chemistry Research, 2001.
885 **40**(9): p. 2054-2058.
- 886 129. Shi, X.C., et al., *Synthesis and properties of $\text{Li}_{1.6}\text{Mn}_{1.6}\text{O}_4$ and its adsorption application*.
887 Hydrometallurgy, 2011. **110**(1-4): p. 99-106.
- 888 130. Wang, H.S., et al., *Selective recovery of lithium from geothermal water by EGDE cross-linked*
889 *spherical CTS/LMO*. Chemical Engineering Journal, 2020. **389**(124410).
- 890 131. Wang, L., et al., *Correlation between Li^+ adsorption capacity and the preparation conditions of*
891 *spinel lithium manganese precursor*. Solid State Ionics, 2006. **177**(17-18): p. 1421-1428.
- 892 132. Zandevakili, S., M. Ranjbar, and M. Ehteshamzadeh, *Synthesis of a nanostructure ion sieve with*
893 *improved lithium adsorption capacity*. Micro & Nano Letters, 2014. **9**(7): p. 455-459.
- 894 133. Xu, H., C.-G. Chen, and Y.-H. Song, *Synthesis and Properties of Lithium Ion-sieve Precursor*
895 *$\text{Li}_4\text{Mn}_5\text{O}_{12}$* . Journal of Inorganic Materials, 2013. **28**(7): p. 720-726.
- 896 134. Chung, K.S., et al., *Preparation of ion-sieve type (H) $[\text{M}_{0.5}\text{Mn}_{1.5}]\text{O}_4$ (M=Mg, Zn) and their*
897 *lithium adsorption properties in seawater*. Solid State Phenomena, 2007. **124-126**: p. 739-742.
- 898 135. Chen, M., et al., *Improved performance of Al-doped LiMn_2O_4 ion-sieves for Li^+ adsorption*.
899 Microporous and Mesoporous Materials, 2018. **261**: p. 29-34.
- 900 136. Cao, G.F., et al., *Synthesis, Adsorption Properties and Stability of Cr-Doped Lithium Ion Sieve in*
901 *Salt Lake Brine*. Bulletin of the Chemical Society of Japan, 2019. **92**(7): p. 1205-1210.
- 902 137. Qiu, Z., et al., *$\text{Li}_4\text{Mn}_5\text{O}_{12}$ doped cellulose acetate membrane with low Mn loss and high stability*
903 *for enhancing lithium extraction from seawater*. Desalination, 2021. **506**(115003).
- 904 138. Kamran, U. and S.-J. Park, *Hybrid biochar supported transition metal doped MnO_2 composites:*
905 *Efficient contenders for lithium adsorption and recovery from aqueous solutions*. Desalination,
906 2022. **522**(115387).
- 907 139. Qian, F., et al., *Enabling highly structure stability and adsorption performances of $\text{Li}_{1.6}\text{Mn}_{1.6}\text{O}_4$*
908 *by Al-gradient surface doping*. Separation and Purification Technology, 2021. **264**(118433).
- 909 140. Qian, F., et al., *Enhancing the Li^+ adsorption and anti-dissolution properties of $\text{Li}_{1.6}\text{Mn}_{1.6}\text{O}_4$ with*
910 *Fe, Co doped*. Hydrometallurgy, 2020. **193**(105291).
- 911 141. Qian, F., et al., *Trace doping by fluoride and sulfur to enhance adsorption capacity of manganese*
912 *oxides for lithium recovery*. Materials & Design, 2020. **194**(108867).
- 913 142. Qian, F., et al., *K-gradient doping to stabilize the spinel structure of $\text{Li}_{1.6}\text{Mn}_{1.6}\text{O}_4$ for Li^+ recovery*.
914 Dalton Trans, 2020. **49**(31): p. 10939-10948.
- 915 143. Xue, F., et al., *Fe_3O_4 -doped lithium ion-sieves for lithium adsorption and magnetic separation*.
916 Separation and Purification Technology, 2019. **228**(115750).
- 917 144. Su, Y., F. Qian, and Z. Qian, *Enhancing adsorption capacity and structural stability of*
918 *$\text{Li}_{1.6}\text{Mn}_{1.6}\text{O}_4$ adsorbents by anion/cation Co-doping*. RSC Advances, 2022. **12**(4): p. 2150-2159.
- 919 145. Bajestani, M.B., A. Moheb, and M. Masigol, *Simultaneous Optimization of Adsorption Capacity*
920 *and Stability of Hydrothermally Synthesized Spinel Ion Sieve Composite Adsorbents for Selective*

- 921 *Removal of Lithium from Aqueous Solutions*. Industrial & Engineering Chemistry Research, 2019.
 922 **58**(27): p. 12207-12215.
- 923 146. Luo, G., et al., *Electrochemical lithium ions pump for lithium recovery from brine by using a*
 924 *surface stability Al₂O₃-ZrO₂ coated LiMn₂O₄ electrode*. Journal of Energy Chemistry, 2022. **69**: p.
 925 244-252.
- 926 147. Hong, H.-J., et al., *Macroporous Hydrogen Manganese Oxide/Al₂O₃ for Effective Lithium*
 927 *Recovery from Seawater: Effects of the Macropores vs Mesopores*. Industrial & Engineering
 928 Chemistry Research, 2019. **58**(19): p. 8342-8348.
- 929 148. Hong, H.-J., et al., *Highly porous and surface-expanded spinel hydrogen manganese oxide*
 930 *(HMO)/Al₂O₃ composite for effective lithium (Li) recovery from seawater*. Chemical Engineering
 931 Journal, 2018. **337**: p. 455-461.
- 932 149. Hong, H.-J., et al., *Immobilization of hydrogen manganese oxide (HMO) on alpha-alumina bead*
 933 *(AAB) to effective recovery of Li⁺ from seawater*. Chemical Engineering Journal, 2015. **271**: p.
 934 71-78.
- 935 150. Han, Y., H. Kim, and J. Park, *Millimeter-sized spherical ion-sieve foams with hierarchical pore*
 936 *structure for recovery of lithium from seawater*. Chemical Engineering Journal, 2012. **210**: p.
 937 482-489.
- 938 151. Ryu, T., et al., *Recovery of Lithium Ions from Seawater Using a Continuous Flow Adsorption*
 939 *Column Packed with Granulated Chitosan–Lithium Manganese Oxide*. Industrial & Engineering
 940 Chemistry Research, 2016. **55**(26): p. 7218-7225.
- 941 152. Wang, Y., et al., *Mesoporous hollow silicon spheres modified with manganese ion sieve:*
 942 *Preparation and its application for adsorption of lithium and rubidium ions*. Applied
 943 Organometallic Chemistry, 2017. **32**(3): p. 4182-4193.
- 944 153. Ryu, T., et al., *Mechanochemical synthesis of silica-lithium manganese oxide composite for the*
 945 *efficient recovery of lithium ions from seawater*. Solid State Ionics, 2017. **308**: p. 77-83.
- 946 154. Recepoglu, Y.K., et al., *Equilibrium and Kinetic Studies on Lithium Adsorption from Geothermal*
 947 *Water by lambda-MnO₂*. Solvent Extraction and Ion Exchange, 2017. **35**(3): p. 221-231.
- 948 155. Chaban, M.A., et al., *Selectivity of new inorganic ion-exchangers based on oxides of titanium and*
 949 *manganese at sorption of lithium from aqueous media*. Journal of Water Chemistry and
 950 Technology, 2016. **38**(1): p. 8-13.
- 951 156. Xiao, J., et al., *Lithium ion adsorption-desorption properties on spinel Li₄Mn₅O₁₂ and pH-*
 952 *dependent ion-exchange model*. Advanced Powder Technology, 2015. **26**(2): p. 589-594.
- 953 157. Guo, Z.-Y., et al., *Electrochemical lithium extraction based on “rocking-chair” electrode system*
 954 *with high energy-efficient: The driving mode of constant current-constant voltage*. Desalination,
 955 2022. **533**(115767).
- 956 158. Jung, S.Y., et al., *Electrode design and performance of flow-type electrochemical lithium*
 957 *recovery (ELR) systems*. Desalination, 2022. **532**(115732).
- 958 159. Xu, W., L. He, and Z. Zhao, *Lithium extraction from high Mg/Li brine via electrochemical*
 959 *intercalation/de-intercalation system using LiMn₂O₄ materials*. Desalination, 2021. **503**(114935).
- 960 160. Mu, Y., et al., *Electrochemical lithium recovery from brine with high Mg²⁺/Li⁺ ratio using*
 961 *mesoporous λ-MnO₂/LiMn₂O₄ modified 3D graphite felt electrodes*. Desalination, 2021.
 962 **511**(115112).
- 963 161. Shi, X.-c., et al., *Synthesis of Li⁺ adsorbent (H₂TiO₃) and its adsorption properties*. Transactions
 964 of Nonferrous Metals Society of China, 2013. **23**(1): p. 253-259.
- 965 162. Wang, S., et al., *Selective adsorption of lithium from high Mg-containing brines using H_xTiO₃ ion*
 966 *sieve*. Hydrometallurgy, 2017. **174**: p. 21-28.
- 967 163. Safari, S., B.G. Lottermoser, and D.S. Alessi, *Metal oxide sorbents for the sustainable recovery*
 968 *of lithium from unconventional resources*. Applied Materials Today, 2020. **19**(100638).
- 969 164. Chitrakar, R., et al., *Lithium recovery from salt lake brine by H₂TiO₃*. Dalton Trans, 2014. **43**(23):
 970 p. 8933-8939.

- 971 165. Kataoka, K., et al., *Crystal growth and structure refinement of monoclinic Li₂TiO₃*. Materials
972 Research Bulletin, 2009. **44**(1): p. 168-172.
- 973 166. He, G., et al., *The optimal condition for H₂TiO₃-lithium adsorbent preparation and Li⁺
974 adsorption confirmed by an orthogonal test design*. Ionics, 2015. **21**(8): p. 2219-2226.
- 975 167. Marthi, R., et al., *On the Structure and Lithium Adsorption Mechanism of Layered H₂TiO₃*. ACS
976 Appl Mater Interfaces, 2021. **13**(7): p. 8361-8369.
- 977 168. Yi, T.-F., S.-Y. Yang, and Y. Xie, *Recent advances of Li₄Ti₅O₁₂ as a promising next generation
978 anode material for high power lithium-ion batteries*. Journal of Materials Chemistry A, 2015.
979 **3**(11): p. 5750-5777.
- 980 169. Sun, X., P.V. Radovanovic, and B. Cui, *Advances in spinel Li₄Ti₅O₁₂ anode materials for lithium-
981 ion batteries*. New Journal of Chemistry, 2015. **39**(1): p. 38-63.
- 982 170. Zhang, L., et al., *Preparation of H₂TiO₃-lithium adsorbent by the sol-gel process and its
983 adsorption performance*. Applied Surface Science, 2016. **368**: p. 82-87.
- 984 171. Moazeni, M., et al., *Hydrothermal synthesis and characterization of titanium dioxide nanotubes
985 as novel lithium adsorbents*. Materials Research Bulletin, 2015. **61**: p. 70-75.
- 986 172. Wang, S., et al., *Hydrothermal synthesis of lithium-enriched β-Li₂TiO₃ with an ion-sieve
987 application: excellent lithium adsorption*. RSC Advances, 2016. **6**(104): p. 102608-102616.
- 988 173. Hossain, S.M., et al., *Preparation of effective lithium-ion sieve from sludge-generated TiO₂*.
989 Desalination, 2022. **525**(115491).
- 990 174. Gu, D., et al., *Lithium ion sieve synthesized via an improved solid state method and adsorption
991 performance for West Taijinar Salt Lake brine*. Chemical Engineering Journal, 2018. **350**: p. 474-
992 483.
- 993 175. Zhang, L., et al., *Effect of crystal phases of titanium dioxide on adsorption performance of
994 H₂TiO₃-lithium adsorbent*. Materials Letters, 2014. **135**: p. 206-209.
- 995 176. Zhang, L., et al., *Synthesis of H₂TiO₃-lithium adsorbent loaded on ceramic foams*. Materials
996 Letters, 2015. **145**: p. 351-354.
- 997 177. Zhao, B., et al., *Hydrothermal synthesis and adsorption behavior of H₄Ti₅O₁₂ nanorods along
998 [100] as lithium ion-sieves*. RSC Advances, 2020. **10**(58): p. 35153-35163.
- 999 178. Shoghi, A., et al., *Spinel H₄Ti₅O₁₂ nanotubes for Li recovery from aqueous solutions:
1000 Thermodynamics and kinetics study*. Journal of Environmental Chemical Engineering, 2021.
1001 **9**(104679).
- 1002 179. Zhang, L.-Y., et al., *Preparation of Ni-Doped Li₂TiO₃ Using an Inorganic Precipitation-
1003 Peptization Method*. Coatings, 2019. **9**(11).
- 1004 180. Wang, S., et al., *High adsorption performance of the Mo-doped titanium oxide sieve for lithium
1005 ions*. Hydrometallurgy, 2019. **187**: p. 30-37.
- 1006 181. Wang, S., et al., *Superior lithium adsorption and required magnetic separation behavior of iron-
1007 doped lithium ion-sieves*. Chemical Engineering Journal, 2018. **332**: p. 160-168.
- 1008 182. Miao, J., et al., *Novel LIS-doped mixed matrix membrane absorbent with high structural stability
1009 for sustainable lithium recovery from geothermal water*. Desalination, 2022. **527**(115570).
- 1010 183. Lawagon, C.P., et al., *Development of high capacity Li⁺ adsorbents from H₂TiO₃/polymer
1011 nanofiber composites: Systematic polymer screening, characterization and evaluation*. Journal of
1012 Industrial and Engineering Chemistry, 2019. **70**: p. 124-135.
- 1013 184. Lin, H., et al., *Synthesis of Polyporous Ion-Sieve and Its Application for Selective Recovery of
1014 Lithium from Geothermal Water*. ACS Appl Mater Interfaces, 2019. **11**(29): p. 26364-26372.
- 1015 185. Limjuco, L.A., et al., *H₂TiO₃ composite adsorbent foam for efficient and continuous recovery of
1016 Li⁺ from liquid resources*. Colloids and Surfaces A: Physicochemical and Engineering Aspects,
1017 2016. **504**: p. 267-279.
- 1018 186. Marthi, R. and Y.R. Smith, *Application and limitations of a H₂TiO₃ – Diatomaceous earth
1019 composite synthesized from titania slag as a selective lithium adsorbent*. Separation and
1020 Purification Technology, 2021. **254**(117580).

- 1021 187. Zhang, Y., et al., *Preparation of granular titanium-type lithium-ion sieves and recyclability*
1022 *assessment for lithium recovery from brines with different pH value*. Separation and Purification
1023 Technology, 2021. **267**(118613).
- 1024 188. Chen, S., et al., *Titanium-based ion sieve with enhanced post-separation ability for high*
1025 *performance lithium recovery from geothermal water*. Chemical Engineering Journal, 2021.
1026 **410**(128320).
- 1027 189. Wei, S., et al., *Porous lithium ion sieves nanofibers: General synthesis strategy and highly*
1028 *selective recovery of lithium from brine water*. Chemical Engineering Journal, 2020.
1029 **379**(122407).
- 1030 190. Qian, H., et al., *HTO/Cellulose Aerogel for Rapid and Highly Selective Li⁺ Recovery from*
1031 *Seawater*. Molecules, 2021. **26**(4054).
- 1032 191. Tang, L., et al., *High-Density Microporous Li₄Ti₅O₁₂ Microbars with Superior Rate Performance*
1033 *for Lithium-Ion Batteries*. Adv. Sci., 2017. **4**(5): p. 1600311.
- 1034 192. Zhu, X., et al., *Study on adsorption extraction process of lithium ion from West Taijinar brine by*
1035 *shaped titanium-based lithium ion sieves*. Separation and Purification Technology, 2021.
1036 **274**(119099).
- 1037 193. Li, X., et al., *Amorphous TiO₂-Derived Large-Capacity Lithium Ion Sieve for Lithium Recovery*.
1038 Chemical Engineering & Technology, 2020. **43**(9): p. 1784-1791.
- 1039 194. Lawagon, C.P., et al., *Adsorptive Li⁺ mining from liquid resources by H₂TiO₃: Equilibrium,*
1040 *kinetics, thermodynamics, and mechanisms*. Journal of industrial and engineering chemistry,
1041 2016. **35**: p. 347-356.
- 1042 195. Ooi, K., et al., *Modelling of column lithium desorption from Li⁺-loaded adsorbent obtained by*
1043 *adsorption from salt brine*. Hydrometallurgy, 2017. **169**: p. 31-40.
- 1044 196. Li, X., et al., *Taming wettability of lithium ion sieve via different TiO₂ precursors for effective Li*
1045 *recovery from aqueous lithium resources*. Chemical Engineering Journal, 2020. **392**(123731).
- 1046 197. Ji, Z.-Y., et al., *Preparation of titanium-base lithium ionic sieve with sodium persulfate as eluent*
1047 *and its performance*. Chemical Engineering Journal, 2017. **328**: p. 768-775.
- 1048 198. Zhang, L.-Y., et al., *A novel study on preparation of H₂TiO₃-lithium adsorbent with titanyl sulfate*
1049 *as titanium source by inorganic precipitation-peptization method*. RSC Advances, 2018. **8**(3): p.
1050 1385-1391.
- 1051 199. Wang, S., et al., *Application of citric acid as eluting medium for titanium type lithium ion sieve*.
1052 Hydrometallurgy, 2019. **183**: p. 166-174.
- 1053 200. Wang, S., et al., *Lithium adsorption from brine by iron-doped titanium lithium ion sieves*.
1054 Particology, 2018. **41**: p. 40-47.
- 1055 201. Jang, Y. and E. Chung, *Adsorption of Lithium from Shale Gas Produced Water Using Titanium*
1056 *Based Adsorbent*. Industrial & Engineering Chemistry Research, 2018. **57**(25): p. 8381-8387.
- 1057 202. Liu, J., et al., *Alkaline Resins Enhancing Li⁺/H⁺ Ion Exchange for Lithium Recovery from Brines*
1058 *Using Granular Titanium-Type Lithium Ion-Sieves*. Industrial & Engineering Chemistry
1059 Research, 2021. **60**(45): p. 16457-16468.
- 1060 203. Li, N., et al., *Yolk-shell structured composite for fast and selective lithium ion sieving*. J Colloid
1061 Interface Sci, 2018. **520**: p. 33-40.
- 1062 204. Tian, L., W. Ma, and M. Han, *Adsorption behavior of Li⁺ onto nano-lithium ion sieve from hybrid*
1063 *magnesium/lithium manganese oxide*. Chemical Engineering Journal, 2010. **156**(1): p. 134-140.
- 1064 205. Liu, D.-F., S.-Y. Sun, and J.-G. Yu, *Li₄Mn₅O₁₂ Desorption Process with Acetic Acid and Mn*
1065 *Dissolution Mechanism*. Journal of Chemical Engineering of Japan, 2019. **52**(3): p. 274-279.
- 1066 206. Ooi, K., et al., *Modelling of column lithium adsorption from pH-buffered brine using surface*
1067 *Li⁺/H⁺ ion exchange reaction*. Chemical Engineering Journal, 2016. **288**: p. 137-145.
- 1068 207. Chitrakar, R., et al., *Synthesis of Iron-Doped Manganese Oxides with an Ion-Sieve Property:*
1069 *Lithium Adsorption from Bolivian Brine*. Industrial & Engineering Chemistry Research, 2014.
1070 **53**(9): p. 3682-3688.

- 1071 208. Jun Ge, J.S., Shuang Wu, *Lithium extraction from Salt lakes in China towards maturity*. 2021,
1072 Minerals Securities Co. LTD: Nonferrous metals.
- 1073 209. HE Yongping, Y.X., WANG Wenhai, Xing Hong, Jin Shengjun, WANG Shijiao, ZHANG
1074 Rongzi, MAO Xinyu, CHEN Caixia, ZHANG Guicheng, *The preparation method and lithium*
1075 *adsorbent of a kind of lithium adsorbent*, C. Patent, Editor. 2017, Qinghai Salt Lake Industry Co
1076 Ltd: China.
- 1077 210. WANG Wenhai, X.H., ZHU Hongwei, MAO Xinyu, ZHANG Chengsheng, YANG Jianyu,
1078 ZHANG Zhanwei, ZHANG Shengshun, DING Zhihai, JIN Caiying, *Method for restoring*
1079 *property of lithium adsorbent*, C. Patent, Editor. 2014, Qinghai Salt Lake Industry Co Ltd: China.
- 1080 211. HE Yongping, X.H., ZHANG Zhanwei, WANG Wenhai, WANG Xingfu, XIE Kangmin, WANG
1081 Shijun, MAO Xinyu, YANG Jianyu, QI Wei, SUN Yonglong, MA Cunbiao, ZHANG Rongzi,
1082 SONG Shengzhong, CHEN Caixia, ZHANG Chengsheng, *A kind of new process of salt lake*
1083 *bittern production high-purity lithium chloride*, C. Patent, Editor. 2017, Qinghai Salt Lake
1084 Industry Co Ltd: China.
- 1085 212. HE Yongping, X.H., SUN Yonglong, WANG Wenhai, ZHANG Chengsheng, YANG Jianyu,
1086 ZHANG Rongzi, SONG Shengzhong, ZHANG Zhanwei, HE Xiaojun, ZHU Xujia, DENG
1087 Yuxing, ZHANG Junxian, ZHANG Chengyong, CHEN Caixia, *Method and device for preparing*
1088 *high-lithium mother liquor by using old brine through adsorption method*, C. Patent, Editor.
1089 2021, Qinghai Salt Lake Fozhao Lanke Lithium Industry Co ltd Qinghai Salt Lake Industry Co
1090 Ltd: China.
- 1091 213. HE Yongping, X.H., YANF Jianyu, WANG Wenhai, MAO Xinyu, YAN Xiongzong, ZHANG
1092 Zhanwei, MA Cunbiao, ZHANG Rongzi, ZHANG Chengsheng, QI Wei, SUN Yonglong, HE
1093 Xiaojun, ZHAO Yonggui, JIN Caiying, HAN Sheng, *A kind of new process and equipment of salt*
1094 *lake bittern production lithium chloride*, C. Patent, Editor. 2017, Qinghai Salt Lake Industry Co
1095 Ltd: China.
- 1096 214. Shun Li, Z.X., Dalin Liu, Chengyong Zhang, *Record sheet of Investor Relations activities of*
1097 *Qinghai Salt Lake Industry Co.,Ltd in Jul. 2021*, G.W. Huayu Wu, Hong Wang, Zhenwei Zhang,
1098 Wenjie Zhang, Hao Li, Teng Zhang, Qi Zhang, Xin Jin, Xin Wan, Editor. 2021, * ST Saltlake.
- 1099 215. Shun Li, Z.X., Jianyu Yang, Dalin Liu, *Record sheet of Investor Relations activities of Qinghai*
1100 *Salt Lake Industry Co.,Ltd in Sep. 2021*, J.C. Guomeng Sun, Feng Zhang, Chongxin Zhang, Ke
1101 Yang, Qian Wang, Mingsong Jiang, Editor. 2021, Saltlake shares.
- 1102 216. Patrick, W., *Techno-Economic Analysis of Lithium Extraction from Geothermal Brines*. 2021,
1103 Golden, CO: National Renewable Energy Laboratory. NREL/TP-5700-79178.

1104